NTNU – Trondheim
Norwegian University of
Science and Technology

Multiphase Flow in Porous Media

Farad Kamyabi

Petroleum Engineering
Submission date: June 2014
Supervisor: Jon Kleppe, IPT
Co-supervisor: Geir Berge, Petrell AS

Norwegian University of Science and Technology
Department of Petroleum Engineering and Applied Geophysics

NTNU
Norwegian University of Science and Technology

petrell

Multiphase Flow in Porous Media

TPG4920 – Petroleum Engineering, Master Thesis

Farad Kamyabi

MASTER THESIS SUBMITTED TO THE DEPARTMENT OF PETROLEUM ENGINEERING AND APPLIED GEOPHYSICS IN PARTIAL FULFILLMENT OF THE REQUIREMENTS FOR THE DEGREE OF MASTER OF SCIENCE IN PETROLEUM ENGINEERING

Trondheim, Norway
June 2014

Abstract

In the hydrocarbon reservoirs that are normally saturated with two or more fluids, in order for better description of the flowing fluids behaviors and rock–fluid interaction, the concept of relative permeability and capillary pressure should be exploited.

Brilliant by Petrell AS is an object-oriented (C++) multi-physics Computational Fluid Dynamics (CFD) package developed for simulation of flow. In the continuous process of improving the system, the aim of this work[1] is to model the multiphase flow through porous media using Darcy's equation. The models in the developed code are based on the conservation equation for each mass to obtain the pressure and saturation fields. After the code is benchmarked against the results from Eclipse for the simulation of single-phase flow, another phase is added to the porous flow part of the code to perform the simulation of multiphase flow through porous media. In this process, first the transmissibilities in the already implemented FVM code have been corrected. Then capillary pressure equations and different relative permeability models have been added to the code. Two test cases, one self-constructed and one from SPE cases, are used to compare the performances of the implemented code and Eclipse. Simulation results are then shown for different relative permeability model.

Table of Contents

Table of Figures

List of Tables

Nomenclature

Following is the list of symbols used in this thesis and might come in handy if the reader is not familiar with the notations.

A	Cross-sectional area
a	Speed of sound
C	Courant number
c	Compressibility
E, W, N, S, F, B	East, west, north, south, forward, backward neighboring CVs' central nodes
e, w, n, s, f, b	East, west, north, south, forward, backward face of a control volume
$\vec{\mathrm{F}}$	Differentiable vector field
g	Acceleration of gravity
K	Equilibrium-constant
k	Absolute permeability
M	Molecular weight
$\vec{n}$	Normal vector
N_p	Number of phases
P	Node in the center of control volume
p_c	Capillary pressure
p	Global pressure
q	External mass flow rate
R	Universal gas constant
$\mathrm{R_s}$	Solution gas-oil ratio
S	Surface
S_{iw}	Irreducible water saturation
S_{wn}	Normalized water saturation
S_α	Saturation of phase α
$S_{\alpha r}$	Residual saturation
T	Temperature
T_α	Transmissibility for phase α
$\vec{\mathrm{u}}$	Velocity vector
V	Volume
V_m	Molar volume
x	Oil phase mole fraction
y	Gas phase mole fraction
β	Water-oil volumetric fraction
Δt	Timestep ($\Delta t = t^{n+1} - t^n$)
ϕ	Porosity
λ	Total mobility
μ	Dynamic viscosity
ν	Specific volume
ρ, ρ_α	Density, phase density
σ	Surface tension

ω	Acentric factor
ξ	Mobility ratio
$\overline{\overline{\nabla}}$	Divergence (Del) operator
∂	Differential operator

Subscripts

avg	Average
b	Bulk volume
c	Critical property
D	Displacing phase
d	Displaced phase
g	Gas phase
i	Component index
l	Liquid phase
max	Maximum
n	Nonwetting phase
o	Oil phase
p	Pore volume
r	Reduced property
w	Water phase
x	x-direction
y	y-direction
z	z-direction
α	Phase index
ω	Wetting phase

Superscripts

n	Old timestep
$\mathrm{n}+1$	Current (or new) timestep

Abbreviations

AIM	Adaptive Implicit Method
CV	Control volume
FDM	Finite Difference Method
FEM	Finite Element Method
FI	Fully Implicit
FVM	Finite Volume Method
IMPES	Implicit pressure-Explicit Saturation
$Relperm$	Relative permeability
$\mathrm{PR}-\mathrm{EOS}$	Peng-Robinson Equation of State
PVT	Pressure–Volume–Temperature

Preface

This is a master thesis in the field of Petroleum Engineering. It is written for Petrell AS and the Department of Petroleum Engineering and Applied Geophysics at Norwegian University of Science and Technology (NTNU). The work counts for 30 credits equivalent to a full semester of work.

About Petrell

Petrell AS is a small company with only about 15 employees, based in Trondheim whose main area of focus includes multiphysics process simulations with its own two commercially available computer software, Brilliant and VessFire. They do consultancy services within fire safety design, gas dispersion and process systems safety in addition to general safety studies and risk analysis [1]. The clients are many of the large petroleum companies around the world.

Petrell AS is a commercial company which means that sensitive information is confidential. This means that the code I have developed is the property of Petrell AS and should not be distributed outside the company. Although the theory behind is available. This has not affected my work in any way.

Acknowledgements

I would like to express my gratitude to my supervisor Professor Jon Kleppe for giving me the opportunity to undertake this study and for guidance and support throughout the course of this work.

I am grateful for the privilege to work with Dr. Geir Berge who has provided me with excellent professional guidance throughout this study and also the opportunity to experience practical reservoir engineering.

I am also very grateful to all my friends at Petrell AS for their good friendship and continuous encouragement. Among those, I would like to give my sincere thanks to Eirik Marthinsen for all the excellent advice and enlightened discussions. The discussions with Eirik always broaden my mind and provide helpful insight from a new point of view. I also wish to thank Anders Granskogen Bjørnstad for the help on the problems with the thermodynamics, and Dr. Torgeir Stensrud Ustad and Torstein Hegge for their suggestions for the thesis.

Farad Kamyabi
Trondheim, June 2014

This page intentionally left blank.

1 Introduction

The correct description of flow and transport in porous media is a matter of great involvedness with a long, rich history in different fields of study such as fluid mechanics, heat transfer and petroleum engineering. Important technological applications involving multiphase flow and multicomponent displacement in porous media occur in petroleum engineering, where multiple flowing phases naturally exist in oil reservoirs, and when diverse range of enhanced recovery techniques including water and CO_2 flooding are employed.

1.1 Background and Motivation

Brilliant is a multiphysics simulation system where fluid flow (Computational Fluid Dynamics, CFD) and stress analysis (Finite Element Method, FEM) are seamless integrated. Fluid flow includes both flow in pipes and flow in porous media. The general flow model applied in different simulators is based on the solution of the conservation equations of momentum, mass and energy.

For flow in porous media, the Darcy equation has been applied. The Darcy equation is based on the principle of a linear relation between the velocity and the pressure gradient in the porous media. The linear factor is expressed as porosity and is representing the resistant to flow in a solid media. The flow process in porous media is governed by several physical phenomena such as viscous forces and also the forces coming from surface tensions between solid and fluid, but also surface tensions between different phases of the fluid. The flow process would in principle be best modeled by use of the momentum equation, but it takes more simulation effort to solve the momentum equation than use the Darcy equation. For this reason the Darcy equation is most commonly applied in simulations of fluid flow through porous media.

In this thesis a multiphase model based on Darcy equation has been implemented in Brilliant. The use of relative permeability has also been investigated in advance. For the reason of implementing a new simulation method in Brilliant, it was of interest that the model be tested with simulations performed by means of Eclipse, revised, and possibly improved. During doing this task, one important question in mind was if there are any other methods that could be better and more efficient.

1.2 Multiphase Flow and Porous Media

Porous media modeling demands thorough explanation of rock and fluid properties. The tortuous structure of porous media naturally contributes to complicated fluid transport through the pores. Since there is no interaction between fluids, single phase flow is comparatively easy to visualize. In this kind of system, flow efficiency is a function of permeability which is a property of rock and independent of the fluid saturating it. Single phase fluid flow through a

porous medium is well described by Darcy's law, and the primary elements of the subject have been well understood for 150 years.

Multiphase flow through porous media is important for a various applications such as CO_2 sequestration, and enhanced oil recovery. These often involve the displacement of a non-wetting invading fluid from a porous medium by a wetting fluid, a physical phenomenon known as imbibition. Modeling of multiphase flow, on the other hand is still an enormous technical challenge. To capture the best model of multiphase flow, true description of fluid interaction such as capillary pressure and relative permeability is inevitable. Considering these parameters, the complexity of numerical calculation in reservoir simulation process will increase. In some cases, these two parameters will create instability in numerical simulation.

Numerical analysis of multiphase flow has long been a subject of interest, and there exists a growing body of literature addressing this subject. The modeling of such physical flow process mainly requires solving the mass and momentum conservation equations associated with equations of capillary pressure p_c, saturation S and relative permeability k_r.

1.3 About Brilliant

Brilliant by Petrell AS is an object-oriented (C++) multi-physics Computational Fluid Dynamics (CFD) package developed for simulation of flow and heat transport, including chemical reactions and solid materials [1]. In Brilliant, fluid mixtures including up to 20 components can be covered. It is used to analyze physical phenomena and their consequences including gas dispersion, fluid flow and etc. It treats *compressible* and *incompressible time-dependent* fluid flow as well as *conduction in solid material*. Brilliant has been verified through laboratory tests and benchmarking with FEM codes [2].

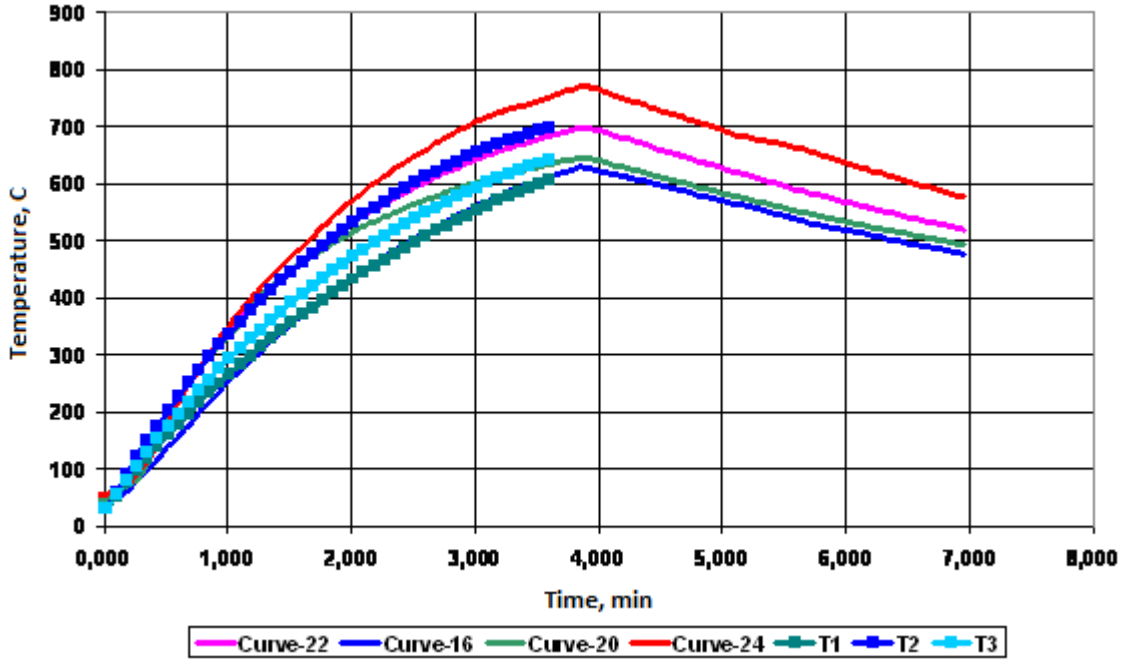

Figure 1.1: Benchmarking Brilliant code with laboratory tests and FEM codes.

In order to run a simulation with Brilliant, a model has to be detailed within a programming language specially made for Brilliant. This requires the definition of the geometry, physical phenomena, and the production or injection scenario. These files themselves should be defined inside the admin file together with the timesteps, maximum simulation time, output file name and courant number.

The geometry of the model is built by combination of hexahedron shaped control volumes. The compiled 3D geometry of the model can be shown in one of the windows within the program. To specify the equation and physical phenomena for each CV, a model has to be defined for that. The materials within the CVs (liquid, gas or solid) are outlined either in the geometry file or another file called scenario file where the content of initial and boundary conditions for each defined models are assigned.

Figure 1.2 illustrates a screen shot of the Brilliant environment. This simulation contains two models: (1) a model for the porous media, the so-called *porosityflow* model, and (2) a model for the fluid flow called *flow* model

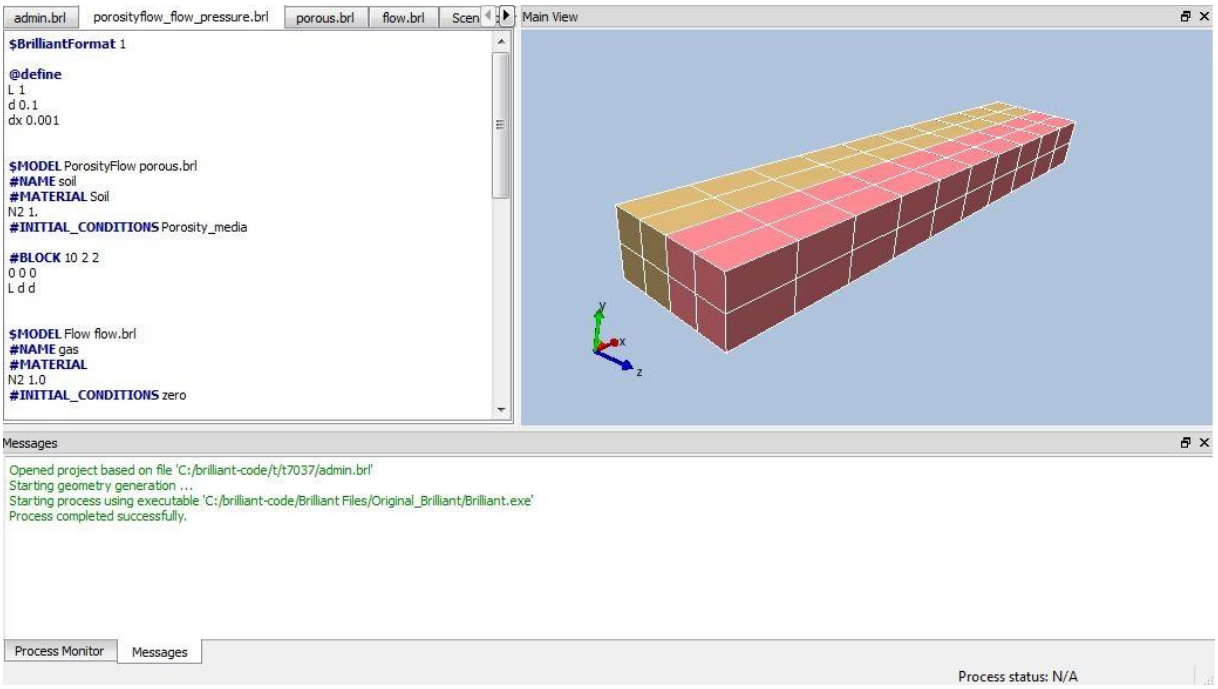

Figure 1.2: The 3D visualization software for building and visualizing the models used in Brilliant. On the right side, the geometry window showing a rectangular with a different color for each model. On the left, the text editor where the commands are put in. The messages, warnings and errors are shown in the bottom window.

1.3.1 Porous Media Model

Among the several models existing in Brilliant, pressure models in reservoir rocks, which have their basis on Navier-Stokes and Darcy's equations, have been capable of modeling only single phase fluid flow up to now. With that in mind, the aim of this work was to put the challenge of implementing multiphase flow in porous media into perspective.

1.4 Thesis Objectives

This thesis entailed development of a model in Brilliant with which to investigate the behavior of multiphase flow in porous media. This development has been divided into two processes: First, to implement the multiphase flow model in Brilliant, and then to test this model with Eclipse. The primary objectives, beyond the obvious goals of accuracy and stability, were (1) to enable study of fundamental physics; (2) to keep the simulation as general as possible so that the dimensionality of the simulation was not changed through simplifying assumption(s) which could alter the nature of multiphase flow.

The thesis can be divided into three main parts. Part I is entirely devoted to the discussion of the basic theories behind fluid flow which includes the introduction to the equations used in the simulation of porous media. Chapter 3 of this part is written to serve as a short description of numerical simulation techniques. In Part II, the theory is set into practice. Chapter 4 presents the description of the practical work and programming concepts. Numerical results from the implemented code in Brilliant are compared with the results from Eclipse. Summary of this work is provided in chapter 5 of Part III. This part continues with chapter 6 where the plots from the simulations are discussed. The thesis ends with the conclusions and some suggestions for future works on the topic.

Part **I**

Theory and Literature Study

2 Theory

Besides reservoir–rock and –fluid characteristics, rock/fluid interaction strongly affects the multiphase flow behavior through porous media. The major purpose of this chapter is to present a quick overview of these properties. It also covers the basics of reservoir–engineering concepts and laws. The theory is well documented in the books of Fanchi [3] and Ertekin *et al.* [4]. Those books have been of great help in forming the backbone of this chapter. For a more thorough understanding of the concepts provided in this chapter, the reader is referred to the above-mentioned books.

2.1 Rock Properties

This section introduces basic reservoir–rock properties, such as porosity and permeability, which are assumed to be independent of the fluid content, as long as no chemical interaction occurs between rock and fluid. The quantification of these parameters is inevitable for correct characterization of any kind of partially blocked control volume, such as porous media.

2.1.1 Porosity

Porosity is the extent to which pores or spaces exist throughout a medium that can be expressed in terms of either absolute or effective porosity. In petroleum engineering it is used as a measure of storage capacity within rock that might contain hydrocarbon and water.

Quantitatively, the porosity of a reservoir rock is defined as a percentage or fraction of the void volume to that volume of reservoir occupied by solid framework

$$\phi = \frac{V_p}{V_b} \tag{2.1}$$

where V_p is the pore volume, and V_b represent the bulk volume.

2.1.2 Permeability

Permeability of rock refers to the measure of how easily fluids may flow through the pore channels of a rock under some potential gradient. To recover the reserves of a hydrocarbon reservoir, it must not only be porous, but also permeable. Permeability is analogous to conductivity in heat flow and diffusivity in mass transfer.

In an ideal case where the reservoir is assumed to be homogeneous, the rock properties within the formation do not change with the location or direction of flow. This ideal situation never exists, but many formations are close enough to this case and therefore can be considered as homogeneous formation. In reality, however, most reservoirs are not homogeneous in terms of permeability; usually there exists a considerable difference

between vertical and horizontal permeabilities. It is generally accepted that the x– and y–direction permeabilities (k_x and k_y, respectively) are almost equal while the permeability in the z–direction (k_z) is usually less than the horizontal permeabilities (k_x and k_y).

2.2 Fluid Properties

Pressure–Volume–Temperature (PVT) properties are the general term used to describe the behavior of the fluids existing in a hydrocarbon reservoir. Accurate determination of these properties is a requirement for a high-quality reservoir analysis. Due to lack of actual data for these properties, numerous empirical correlations such as the equation of state (EOS) and graphical techniques have been developed to predict PVT properties. However, they are mostly-precise and their parameters have to be tuned to improve the accuracy of these correlations.

PVT properties of interest in reservoir simulation include *fluid compressibility, fluid density, fluid viscosity, formation volume factors of fluid* and *solution gas/liquid ratio*. Among those, the two most important ones of these properties, i.e., *fluid compressibility* and *fluid viscosity* are discussed in this section to gain insight into the role they play in reservoir modeling.

2.2.1 Fluid Compressibility

Fluid compressibility is defined as the fractional volumetric change of a given mass per pressure change under condition of constant temperature. Mathematically, the coefficient of isothermal compressibility can be defined as

$$c = -\frac{1}{V}\left(\frac{\partial V}{\partial p}\right)_T \tag{2.2}$$

where V is volume and p is pressure. The subscript T is used to denote that the partial differentiation is to be taken assuming constant temperature.

In multiphase flow in petroleum reservoirs, water is considered whether as incompressible or slightly compressible while the compressibility of Oil depends on its pressure; if oil pressure is higher than bubblepoint pressure, oil and its solution gas, are treated as slightly compressible and if the pressure falls below bubblepoint pressure, they are considered to be compressible.

Compressibility and Speed of Sound. The speed of sound also known as sonic or acoustic velocity is the rate of propagation of the acoustic waves through a medium. In classical mechanics, the speed of sound *a* is related to the change in pressure and density of the material and is given by Laplace equation

$$a^2 = \frac{\partial p}{\partial \rho} \tag{2.3}$$

In the equation above, p is the pressure and ρ is the density. The derivative is to be taken adiabatically, i.e., at constant entropy.

Equation (2.3) can be written in terms of specific volume ν as

$$a = \sqrt{-\nu^2 \left(\frac{\partial p}{\partial \rho}\right)} \tag{2.4}$$

Substitution of the partial derivative of this equation with the one incorporated in equation (2.2) results in

$$a = \sqrt{\frac{\nu}{c}} = \sqrt{\frac{1}{c\rho}} \tag{2.5}$$

Thus, speed of sound depends on both compressibility and density of the material. It should be pointed out that the relation between speed of sound and compressibility obtained in equation (2.5) can be used to estimate the medium or fluid compressibility.

In 1993, Dong and Gudmundsson [6] proposed a model for the speed of sound in multiphase mixture. They based their calculations on the properties of the mixture. In the case of water and oil mixture in the liquid phase, they defined the liquid density by the following expression

$$\rho_l = \beta\rho_w + (1-\beta)\rho_o \tag{2.6}$$

and liquid compressibility by

$$c_l = \beta c_w + (1-\beta)c_o \tag{2.7}$$

where β is the water-oil volumetric fraction. Subscripts l, w and o indicate the liquid, water and oil phases respectively.

In a system where all three phases (water, oil and gas) exist, the density and compressibility of the mixture are calculated by considering gas-liquid void fraction, α

$$\rho_m = \alpha\rho_g + (1-\alpha)\rho_l \tag{2.8}$$

And

$$c_m = \alpha c_g + (1-\alpha)c_l \tag{2.9}$$

where the subscripts m, g and l indicate the mixture, gas phase and liquid phase respectively.

Combination of equation (2.7) and (2.9) yields

$$c_m = \alpha c_g + (1-\alpha)[\beta c_w + (1-\beta)c_o] \tag{2.10}$$

Speed of sound for the mixture can be deduced from combination of equation (2.10) with the expression of speed of sound in terms of material compressibility and specific heat ratio. This is beyond the scope of this master thesis and therefore, it is preferable to focus on the main objective of this study. The reader is referred to [5] for further details.

2.2.2 Fluid Viscosity

Fluid viscosity is expressed as the fluid property that offers resistance to shear stress. It is a proportionally factor between shear stress and rate of deformation over time

$$\mu = \frac{\tau}{\frac{\partial u}{\partial y}} \tag{2.11}$$

where μ represents the absolute viscosity of fluid. τ and $\frac{\partial u}{\partial y}$ are the shear stress and rate of deformation respectively.

Fluid viscosity is a function of both temperature and pressure. Increasing the liquid temperature weakens the attractive forces present between its molecules and consequently increases the average speed of the molecules. So, as the temperature of a liquid raises, its viscosity decreases. For the gases, increase in temperature provides more interchange of momentum between molecules which results in an increased viscosity. Compared to temperature change which significantly alters the viscosity, the changes induced by pressure have small impact on the viscosity.

2.3 Fluid/Rock Properties

This section focuses on understanding some of the main concepts as prerequisites for modeling multiphase fluid flow through porous media.

2.3.1 Fluid Saturation

Multiphase flow occurs when several phases reside in a control volume simultaneously. These different phases might be related in the way that either a component exists in more than one phase, or the phases can consist of totally different components. It is obvious that presence of different phases within the same volume results in the volume of each phase to be less than the total volume. By definition, the saturation of a fluid is the ratio of the fluid volume to the pore volume

$$S_\alpha = \frac{V_\alpha}{V_p} \tag{2.12}$$

S_α is the saturation of phase. α, V_α and V_p are, respectively, the phase and pore volumes in the system.

The fluid saturation of each phase is a number between 0 and 1. The phase saturations are associated by an additional constraint equation

$$\sum_\alpha S_\alpha = 1 \tag{2.13}$$

where $\alpha = o, w$ or g.

2.3.2 Interfacial Tension

Surface tension is a property of liquids that make the outer layer of the liquid to act as an elastic plate. This property causes the attraction between the molecules of two liquids present on the surface. Surface tension, indicated by σ, is the force per unit length or energy per unit area. It can also be defined as the work needed to create a unit surface between two surfaces. This unit area is referred to as “interface” for liquid-liquid or liquid-solid interactions and as “surface” when one of the two phases is gas.

Each molecule of the fluid is attracted by surrounding molecules. The ones present within the bulk of the fluid experience an equal attraction force in all directions and therefore the resultant force on them is zero. While for the molecules in the surface, there is no balance between the inter– and intra–molecular forces, and as a result, a net force from intermolecular forces tends to pull the molecules on the surface inward. The force required to react against this net inward pull that causes the surface of the material to have smallest possible size is called “interfacial tension” or “surface tension” depending on the interacting phases.

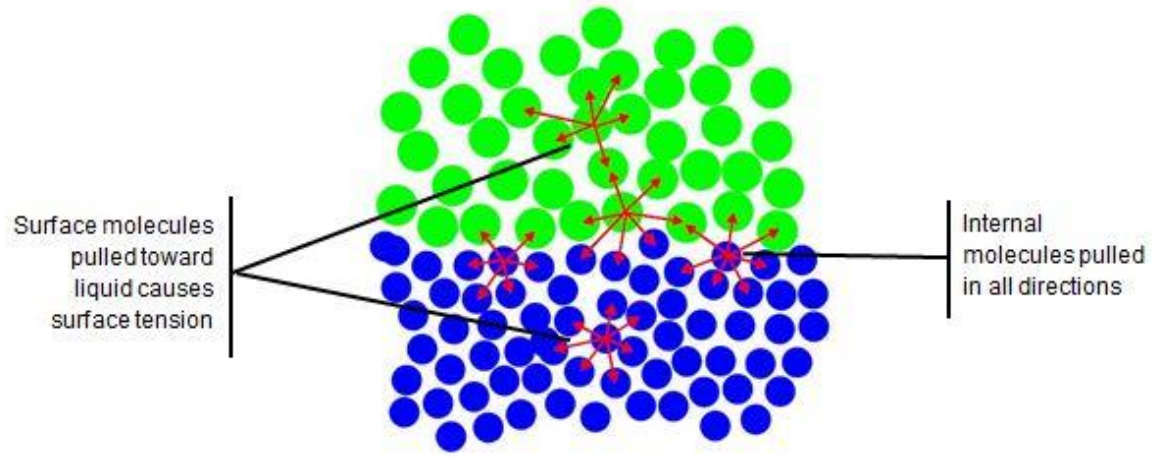

Figure 2.1: Attractive forces between the molecules.

2.3.3 Capillary pressure

Capillary forces in hydrocarbon reservoirs are defined based on the interfacial and surface tensions between the fluids and rocks, the geometry and average size of the pores, and also the wettability of the system. In addition to the above-mentioned items, fluid saturation distribution also controls the curvature of the interface separating two fluids. This curvature tends to form in the smallest possible area. If two immiscible fluids are in interaction, there exists a discontinuity which is a function of the curvature of the interfacing surface. This difference in the pressure across the interface is called capillary pressure p_c. Capillary pressure is, by definition, the pressure difference between the pressure of nonwetting and wetting phases and is always nonzero

$$p_c(S_\omega) = p_n - p_\omega \geq 0 \tag{2.14}$$

where the indices n and ω indicate, respectively, the wetting and nonwetting phase.

Water is always the wetting phase in both water–oil and water–gas or three–phase systems, while gas is considered to be the nonwetting phase all the time. Therefore, the capillary pressure relationship for water-oil system can be written as

$$p_{cow}(S_\omega) = p_o - p_w \tag{2.15}$$

where the subscripts o and w represents the oil and water phases, respectively. Fig. 2.2 represents a typical $p_c - S_w$ curve. S_{w_i} is the so-called irreducible water saturation which is the minimum achievable water saturation.

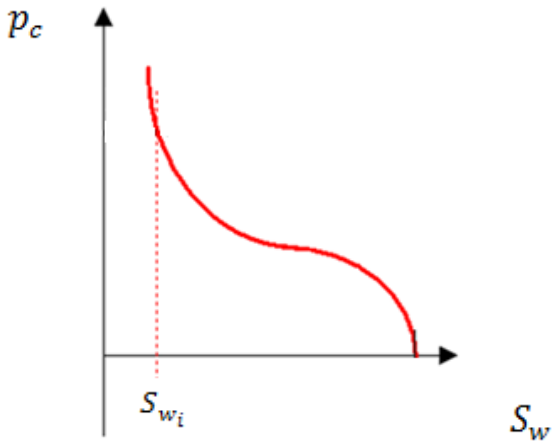

Figure 2.2: typical $p_c - S_w$ curve.

The concept of capillary pressure in reservoir engineering is important for several reasons: (1) determination of the initial fluid distribution in the reservoir, (2) prediction of the recoverable oil, and (3) input data for the reservoir simulation models.

2.3.4 Relative permeability

Hydrocarbon reservoirs are normally saturated with two or more fluids. Therefore, in order for better description of flowing fluids behaviors and rock–fluid interaction, the concept of absolute permeability should be modified. Decrease in the saturation of one phase results in a decreased permeability of that phase. This decreased permeability is called effective permeability of the phase and is expressed as the ability of a reservoir rock to transmit a fluid as related to its ability to transmit another fluid under the same circumstances. Mathematically, relative permeability (relperm) is the ratio of the effective permeability of one phase at a given saturation to the absolute permeability

$$k_{r\alpha} = \frac{k_\alpha}{k} \tag{2.16}$$

where the subscript $r\alpha$ indicates the relative value of phase α.

In the system of multiphase flow, the sum of relative permeability of the phases is always less than or equal to unity

$$k_{rg} + k_{ro} + k_{rw} \leq 1 \tag{2.17}$$

2.3.5 Mobility

Easiness of the displacement of one fluid by another through a porous medium is controlled through the differences in the ratio of relative permeability and viscosity of that fluid, the so-called "fluid mobility", λ. Fluid mobility depends on both the rock and the fluid and is expressed as

$$\lambda_\alpha = \frac{k_{r\alpha}}{\mu_\alpha} \tag{2.18}$$

where the subscript α represents the phase type.

In the flow of one phase by the other phase, mobility ratio is a key parameter in predicting the behavior of the flowing fluids. It is described as the ratio of displacing fluid mobility to the displaced fluid mobility.

For the two-phase system of water-oil where water is injected into the oil zone to sweep the oil, the mobility ratio may be calculated by

$$\xi = \frac{\lambda_D}{\lambda_d} = \frac{\frac{k_w}{\mu_w}}{\frac{k_o}{\mu_o}} \tag{2.19}$$

The subscripts D and d indicate the displacing and displaced phases.

2.4 Two—Phase Relative Permeability Models

Relative permeability data are amongst the most crucial data for reservoir simulation. These data are generally achieved from core analysis in the laboratories. Non-response and missing data should be approximated properly to conduct a flawless reservoir simulation. This is done through the relative permeability models expressed in mathematical form.

As it is described in the previous section, relative permeability is one of parameters that should be considered for modeling the rock–fluid interaction. Therefore, generating high quality relative permeability curve(s) for correct simulation of the multiphase system is inevitable. These models should be able to generate the relative permeability data under in–situ condition since the parameters such as wettability which have great impact on the relative permeability data will alter through change in the measurement condition.

Numerous algebraic models, such as of those Corey [6], Pirson [7], Naar [8], Mohamed [9] and Honarpour [10], have been proposed to determine the missing relative permeability data from core analysis. These models mostly relate the relative permeability data to water saturation. Ensuing section will address some of these models.

2.4.1 Corey's Two—Phase Model

In 1954, Corey [6] proposed an empirical model for predicting two-phase relative permeability using a limited set of data. The model is in the form of power law relationships and as it suffers from some limitations, it is accepted to be a fairly accurate model.

Corey's relative permeability equations for the oil and water phases, respectively, are approximated by

$$k_{ro} = \left[\frac{1 - S_o}{1 - S_{iw}}\right]^2 \left[1 - \left(\frac{S_o - S_{iw}}{1 - S_{iw}}\right)^2\right] \tag{2.20}$$

$$k_{rw} = \left[\frac{S_w - S_{iw}}{1 - S_{iw}}\right]^4 \tag{2.21}$$

In these expressions,

- S_w and S_o are the water and oil saturation.
- S_{iw} denotes the irreducible water saturation.

As explained in the third section this chapter, water and oil are respectively assumed to be the wetting and nonwetting phases in the water-oil system. Therefore, k_{ro} represents the relative permeability of the nonwetting phase while k_{rw} refers to wetting phase relative permeability.

2.4.2 Naar and Henderson's Two—Phase Model

In the model suggested by Naar and Henderson [8], the equation of relative permeability for the wetting phase is the same as the one given in equation (2.21). The nonwetting phase relative permeability model can be established by the following equation

$$k_{ro} = [1 - 2S_{wn}]^{1.5}[2 - (1 - 2S_{wn})^{0.5}] \tag{2.22}$$

where S_{wn} is the normalized water saturation and is defined as:

$$S_{wn} = \frac{S_w - S_{iw}}{1 - S_{iw}} \tag{2.23}$$

The definition of water phase relative permeability in terms of normalized water saturation follows from equation (2.21) as

$$k_{rw} = {S_{wn}}^4 \tag{2.24}$$

2.4.3 Honarpour's Two—Phase Model

The previous two models described in this section do not specify the type of rock which can be considered as a disadvantage for these models. Although Honarpour's proposed model [10] considers the rock type, but it ignores the difference between mixed and intermediate wettabilities.

Following equations show the relative permeability relationships when the reservoir rock type is sandstone

$$k_{ro} = 0.76067\left[\frac{\left(\frac{S_o}{1-S_{iw}}\right)-S_{or}}{1-S_{or}}\right]^{1.8}\left[\frac{S_o-S_{or}}{1-S_{iw}-S_{or}}\right]^2 + 2.6318\phi(1-S_{or})(S_o-S_{or}) \quad (2.25)$$

$$k_{rw} = 0.035388\left[\frac{S_w-S_{iw}}{1-S_{iw}-S_{or}}\right] - 0.0108074\left[\frac{S_w-S_{or}}{1-S_{iw}-S_{or}}\right]^{2.9} + 0.56556(S_w)^{3.6}(S_w-S_{iw}) \quad (2.26)$$

While

$$k_{ro} = 1.2624\left[\frac{S_o-S_{or}}{1-S_{or}}\right]\left[\frac{S_w-S_{iw}}{1-S_{iw}-S_{or}}\right]^2 \quad (2.27)$$

$$k_{rw} = 0.0020525\left[\frac{S_w-S_{iw}}{\phi^{2.15}}\right] - 0.051371\left[\frac{S_w-S_{iw}}{k^{0.43}}\right] \quad (2.28)$$

give the relative permeabilities for limestone reservoirs. These equations are valid for water-oil system when the rock has more affinity for water, that is, water-wet.

2.5 Gauss divergence theorem

From a mathematical point of view, the surface differential and volume integral forms are equal. These forms can be related through the divergence theorem provided by Gauss.

Let $\vec{F}$ be a continuously differentiable vector field in a solid region V whose boundary surface S has a unit vector $\vec{n}$ for the surface normal. Then according to the divergence theorem

$$\oiint_S (\vec{F}.\vec{n})dS = \iiint_V (\overline{\nabla}\,\vec{F})dV \quad (2.29)$$

where $\overline{\nabla}$ is the del operator.

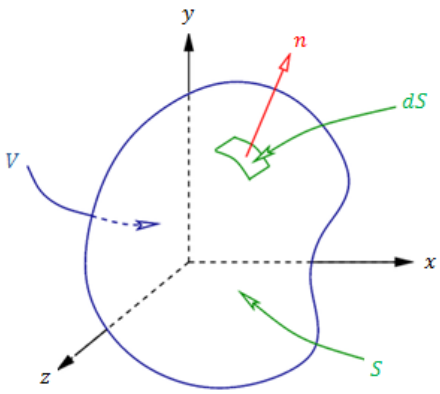

Figure 2.3: Divergence theorem over volume R.

2.6 Law of Mass Conservation

Conservation of mass equation states the balance between rate of mass change in an arbitrary volume and inflow of mass through the boundary surface area S.

On integral form, this balance is expressed as follows

$$\frac{\partial}{\partial t}\iiint_V \rho\phi \, dV + \oiint_S \rho\vec{u}.\vec{n}dS = \iiint_V q \, dV \tag{2.30}$$

where $\overline{\overline{\nabla}}$ is the del operator. q, ρ, $\vec{u}$ and ϕ represent the external mass flow rate, fluid density, velocity vector and porosity, respectively.

The right hand side term of the equation (2.30) can be converted into a volume integral form by the use of the divergence theorem as

$$\oiint_S \rho\vec{u}.\vec{n}dS = \iiint_V \overline{\overline{\nabla}}.(\rho\vec{u})dV \tag{2.31}$$

Thus, for a fixed control volume, the integral form of the conservation law will be

$$\iiint_V \left[\frac{\partial(\rho\phi)}{\partial t} + \overline{\overline{\nabla}}.(\rho\vec{u}) - q\right]dV = 0 \tag{2.32}$$

On the differential form the conservation equation for mass can be written in coordinate invariant form as

$$\frac{\partial(\rho\phi)}{\partial t} + \overline{\overline{\nabla}}.(\rho\vec{u}) = q \tag{2.33}$$

In the multiphase flow, it is necessary to account for the saturation of each phase. Therefore equation (2.33) within each phase α becomes

$$\frac{\partial(\rho_\alpha S_\alpha\phi)}{\partial t} + \overline{\overline{\nabla}}.(\rho_\alpha\vec{u}_\alpha) = q_\alpha \tag{2.34}$$

where α is the phase index.

2.7 Basic Single—Phase—Flow Equation

Combination of mass conservation equation with an appropriate form of momentum equation yields the flow equation. It appears that the best one can do is to use the porous medium analog of Navier-Stokes equation, Darcy's law as the momentum equation

$$\vec{u} = -\frac{k}{\mu}(\overline{\overline{\nabla}}\, p - \rho g\, \overline{\overline{\nabla}}\, z) \tag{2.35}$$

where p is the global pressure, z is the depth below some datum, g is the acceleration gravity, and fluid has permeability k and viscosity μ.

Inserting equation (2.35) into equation (2.33) results in single-phase flow equation

$$\frac{\partial(\rho\phi)}{\partial t} - \overline{\overline{\nabla}}.\left(\rho\frac{k}{\mu}(\overline{\overline{\nabla}}\, p - \rho g\, \overline{\overline{\nabla}}\, z)\right) = q \tag{2.36}$$

2.8 Flow Equations in Mutiphase Flow

To simulate the multiphase flow through porous media, Darcy's law has to be extended to each phase by the same manner done for the single phase flow. For a system of multiphase flow, Darcy's law is stated as

$$\vec{u}_\alpha = -\frac{k k_{r\alpha}}{\mu_\alpha}(\overline{\overline{\nabla}}\, p_\alpha - \rho_\alpha g\, \overline{\overline{\nabla}}\, z) \tag{2.37}$$

In the above equation α indicates the phase type.

In order for a thorough description of the multiphase flow, some additional equations are required to model the interactions between the existing phases. These equations consist of capillary pressure and phase-saturation relationships expressed by equations (2.13) and (2.14).

In describing the fluid flow processes, engineers use either black-oil or compositional model to build an accurate PVT model. Nevertheless, the compositional models are too much complex and require more computational efforts. In contrast, Black-oil PVT models are simpler and do not consider changes in composition of the hydrocarbons by reservoir depletion. As the cost of running a simulation increases with the number of components, the Black-oil model is more preferable to be applied for a reservoir description. The rest of this chapter goes into detail of each of these two models.

2.8.1 Black—Oil Model

These models assume that the hydrocarbons can be labeled as two components, pseudo-oil and pseudo-gas, with constant composition during the modeling period. Water equation in this model is solved explicitly.

The flow equations for the water and oil phases in this model are obtained straightforwardly by substituting equation (2.37) into equation (2.34)

$$\frac{\partial(\rho_w \phi S_w)}{\partial t} - \overline{\overline{\nabla}}.\left(\rho_w \frac{k k_{rw}}{\mu_w}(\overline{\overline{\nabla}}\, p_w - \rho_w g\, \overline{\overline{\nabla}}\, z)\right) = q_w \tag{2.38}$$

$$\frac{\partial(\rho_o \phi S_o)}{\partial t} - \overline{\overline{\nabla}}.\left(\rho_o \frac{k k_{ro}}{\mu_o}(\overline{\overline{\nabla}}\, p_o - \rho_o g\, \overline{\overline{\nabla}}\, z)\right) = q_o \tag{2.39}$$

As for the gas phase, the mass transfer between the oil and/or water, and gas components should be considered in the flow equation. This issue is addressed by gas solubility factor R_s. Gas phase equation, considering mass transfer between oil and gas phases is in the form of

$$\frac{\partial}{\partial t}\left(\rho_g \phi S_g + \rho_o \phi R_s S_o\right) - \overline{\overline{\nabla}}.\left(\rho_g \frac{k k_{rg}}{\mu_g}\left(\overline{\overline{\nabla}}\, p_g - \rho_g g\, \overline{\overline{\nabla}}\, z\right)\right) - \overline{\overline{\nabla}}.\left(\rho_o \frac{k k_{ro} R_s}{\mu_o}(\overline{\overline{\nabla}}\, p_o - \rho_o g\, \overline{\overline{\nabla}}\, z)\right) = q_g + R_s q_g \tag{2.40}$$

In this set of equations, it is assumed that evaporation of oil and water phases in gas is negligible.

2.8.2 Compositional Model

Although the computational effort is a dominant consideration in choosing the PVT model for the flow description, but still the reliability and efficiency of the simulation are important. In the hydrocarbon reservoirs containing light oil, the compositions differ significantly in surface and reservoir conditions. Thus, in addition to pressure, the compositions of the hydrocarbons play a significant role in determination of the fluid phase behavior, and the mass balance equation should be written for each component separately. EOS and K-values can be useful to track the changes of the compositions included in both phases [11].

$$\frac{y_{ig}}{x_{io}} = K_{igo}\left(T, p, C_{ig}, C_{io}\right) \tag{2.41}$$

where K_{igo} shows the state of equilibrium of *i-component* between oil and gas phases. . x_i and y_i indicate mole fraction of component i in oil and gas phases respectively.

Similar to the black-oil modeling, the starting point is writing the continuity equation. As water is treated explicitly, the mass balance equation of water phase is identical to the one in black-oil model expressed in equation (2.38)

$$\frac{\partial(\rho_w \phi S_w)}{\partial t} - \overline{\overline{\nabla}}.\left(\rho_w \frac{k k_{rw}}{\mu_w}(\overline{\overline{\nabla}}\, p_w - \rho_w g\, \overline{\overline{\nabla}}\, z)\right) = q_w \tag{2.38}$$

While for the *i-component* of existing in the hydrocarbons, the flow equation is best described by

$$\frac{\partial}{\partial t}\left[\phi\left(\rho_g y_i S_g + \rho_o x_i S_o\right)\right] - \overline{\overline{\nabla}}.\left(\rho_g y_i \frac{k k_{rg}}{\mu_g}\left(\overline{\overline{\nabla}}\, p_g - \rho_g g\, \overline{\overline{\nabla}}\, z\right)\right) - \overline{\overline{\nabla}}.\left(\rho_o x_i \frac{k k_{ro}}{\mu_o}\left(\overline{\overline{\nabla}}\, p_o - \rho_o g\, \overline{\overline{\nabla}}\, z\right)\right) = q_i \qquad (2.42)$$

Where subscripts i, o and g indicate the component type, oil, and gas phase. x_i and y_i are mole fraction of component i in oil and gas phases respectively.

3 Numerical Simulation of Fluid Flow in Hydrocarbon Reservoirs

The major purpose of this chapter is to describe the methods of solving partial differential equations (PDE). It begins with the definition of frequently used terms in numerical simulation, and then explains two numerical techniques for solving PDEs. Finally, it presents the different linearization schemes mostly applied in hydrocarbon reservoir simulation.

3.1 Terms Used in Numerical Simulation

Since a reservoir engineer spends most of his career dealing with the numerical simulation, he needs to understand its terms properly. This section seeks to describe, as simple and short as possible, several terminologies commonly used in numerical reservoir simulation to convey a general understanding these concepts.

3.1.1 Numerical Method

Finding an exact solution to some differential equations is whether impossible or very time consuming. This is where people employ numerical analysis to address the issue by creating a sequence of approximations. This is done through discretization of the continuous differential equations. Though there exist several methods that offer a means to obtain these approximate solutions, there appears that the most popular ones for the fluid flow equations are the Finite Difference Method (FDM) and Finite Volume Method (FVM) which will be discussed in detail in the next section of this chapter. Numerical stability and the accuracy of the results are the main concern in computer-based simulations.

3.1.2 Gridblock Structure

In numerical simulation, the geometry of the system is divided into a set of smaller shapes, the so-called gridblocks. The structure of these gridblocks can be in 2-D or 3-D Cartesian or cylindrical coordinate whether in simple or curvilinear system depending on the complexity of the system. It is preferred to use larger number of gridblocks for more complex system to acquire high-resolution results from the simulation.

3.1.3 Transmissibility

Transmissibility T measures how easily fluids can flow between two boundary-fitted gridblocks of the simulation grid. The transmissibility term at the interface of two gridblocks for phase α can be defined as:

$$T_\alpha = \left(\frac{kA}{h}\right)_{avg} \left(\frac{k_{r\alpha}}{\mu_\alpha}\right)_{avg} \tag{3.1}$$

As equation (3.1) shows, transmissibility coefficient is a function of the gridblock geometry, absolute and phase relative permeabilities $k_{r\alpha}$, and fluid viscosity of phase α , μ_α. Using the definition of mobility presented in equation (2.18), equation (3.1) reduces to

$$T_\alpha = \left(\frac{kA}{\Delta x}\right)_{avg} (\lambda_\alpha)_{avg} \tag{3.2}$$

Since the phase saturations are significantly dependent upon the mobility terms, choosing the proper way of approximating this item is crucial for a precise simulation. The three existing ways for approximating this term in equation (3.2) are: Upstream selection, weighted average selection, and downstream selection. Among these, upstream mobility selection gives the accurate results, and as for the other two, depending on the gridblock size, the results can be unphysical. Mobility selection is described in greater detail in [12].

3.1.4 Spatial Discretization

Spatial discretization has to do with dividing the continuous simulation region into gridblocks. The size of gridblocks, Δx, is important in the running-time and consistency of the simulation. Depending on the system complexity, the interval lengths can be of a uniform or variable size.

3.1.5 Temporal Discretization

Temporal discretization has to do with dividing the continuous simulation time into smaller timesteps. The same as gridblock size, the size of timesteps, Δt, is also important in the running-time and consistency of the simulation. The fact is that the timestep can neither be too short because of the computation restrictions, nor too big due to the consistency issues.

3.1.6 Numerical Stability

Numerical stability refers to how well a numerical solution of PDEs behaves as the timestep Δt grows. A numerically stable algorithm does not amplify the unavoidable approximation errors for the big sizes of timestep. The solution schemes can be stable, unstable or conditionally stable. For Further details regarding the stability criterion of the numerical solution schemes refer to section 3.3.

3.1.7 Courant Number

Courant number, C defines a condition that is essential for a numerical algorithm to converge. This number is a function of timestep, gridblock size, and the velocity at that gridblock

$$C = \Delta t \sum_{i=1}^{n} \frac{u_{x_i}}{\Delta x_i} \tag{3.3}$$

Where the indices i and n show the current and maximum values of dimension.

The equation above implies that the solution is more stable at small values of Courant number (and therefore timestep), if it is not unconditionally stable.

3.2 Types of Numerical Methods

There are typically three numerical solutions of partial differential equations, namely FDM, FEM and FVM that particularly interest the engineers and scientists. In this section, a short introduction to the two of the above-mentioned numerical solutions of partial differential equations, i.e., FDM and FVM is provided. An excellent introduction into the FDM can be consulted in [13], and the basics of the FVM can be found in the book by Verteeg and Malalasekera [14].

3.2.1 Finite Difference Method (FDM)

In the finite difference method, the derivatives in the PDE are approximated using the Taylor expansion. Forward, backward and central differences are three forms in this method commonly used to obtain the approximations of numerical derivatives.

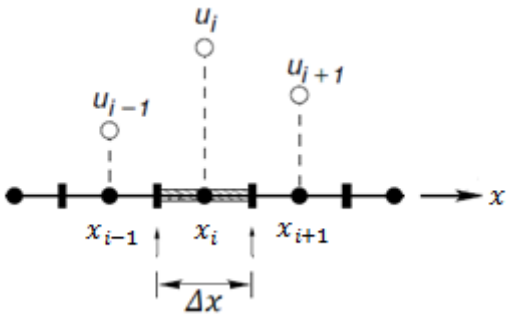

Figure 3.1: Discretized domain for first-order approximation of the derivatives.

As a start, let us consider u is a function of only x. Given the nodal values of $u_i(x)$ as shown in Fig. 3.1, the first-order derivatives of $u_i(x)$ with respect to x have the forms

$$\left(\frac{\partial u}{\partial x}\right)_i = \frac{u_{i+1} - u_i}{\Delta x} - \frac{\Delta x}{2}\left(\frac{\partial^2 u}{\partial x^2}\right)_i - \frac{\Delta x^2}{6}\left(\frac{\partial^3 u}{\partial x^3}\right)_i + \cdots \tag{3.4}$$

for forward difference approximation, and

$$\left(\frac{\partial u}{\partial x}\right)_i = \frac{u_i - u_{i-1}}{\Delta x} + \frac{\Delta x}{2}\left(\frac{\partial^2 u}{\partial x^2}\right)_i - \frac{\Delta x^2}{6}\left(\frac{\partial^3 u}{\partial x^3}\right)_i + \cdots \tag{3.5}$$

for backward difference approximation.

These two approximations are called first-order since the reminders, the marked terms in the two equations above, are in order of $O(\Delta x)$. However, the average of the forward and backward differences, central difference, have the order of $O(\Delta x)^2$. Hence, it is more precise than the other two

$$\left(\frac{\partial u}{\partial x}\right)_i = \frac{u_{i+1} - u_{i-1}}{2\Delta x} - \frac{\Delta x^2}{6}\left(\frac{\partial^3 u}{\partial x^3}\right)_i + \cdots \tag{3.6}$$

Now Finite difference can be expanded to multi-dimensions using the combination of 1D finite difference approximations in different dimensions. For instance, $u(x, y)$ is approximated in 2D by

$$\frac{\partial^2 u}{\partial x \partial y} = \frac{\partial}{\partial x}\left(\frac{\partial u}{\partial y}\right) = \frac{\partial}{\partial y}\left(\frac{\partial u}{\partial x}\right) \tag{3.7}$$

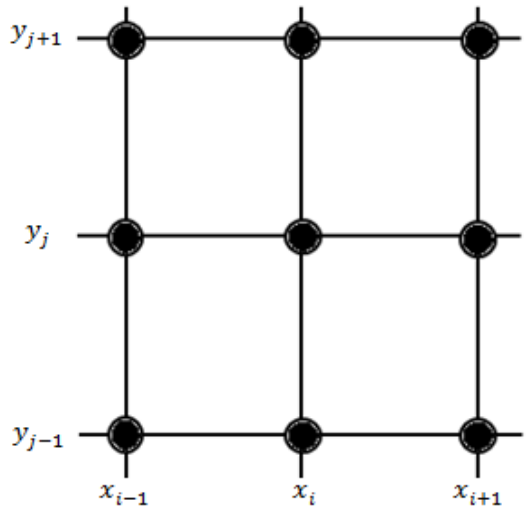

Figure 3.2: Discretized domain for second-order approximation of the derivatives.

When equation (3.4) is substituted into equation (3.7), the following result

$$\left(\frac{\partial^2 u}{\partial x \partial y}\right)_{i,j} = \frac{u_{i+1,j+1} - u_{i+1,j-1} - u_{i-1,j+1} + u_{i-1,j-1}}{4\Delta x \Delta y} \tag{3.8}$$

which is in order of $O[(\Delta x)^2, (\Delta y)^2]$.

It should be noted that the finite differences are applicable for the time derivatives in the exact same manner.

3.2.2 Finite Volume Method (FVM)

The finite volume method is an integration based approach originally developed in order for spatial discretization of the PDEs by computing the numerical flux in and out of the control volume. CVs in FVM can be cell- or vertex-centered.

As shown in Fig. 3.2, FDM uses the values of a variable at each node for calculating the derivatives. However, FVM uses the entire section colored in gray on Fig. 3.3 and calculates the flux across this section. This feature of FVM satisfies the flow conservation as it uses the value of one edge for the next edge.

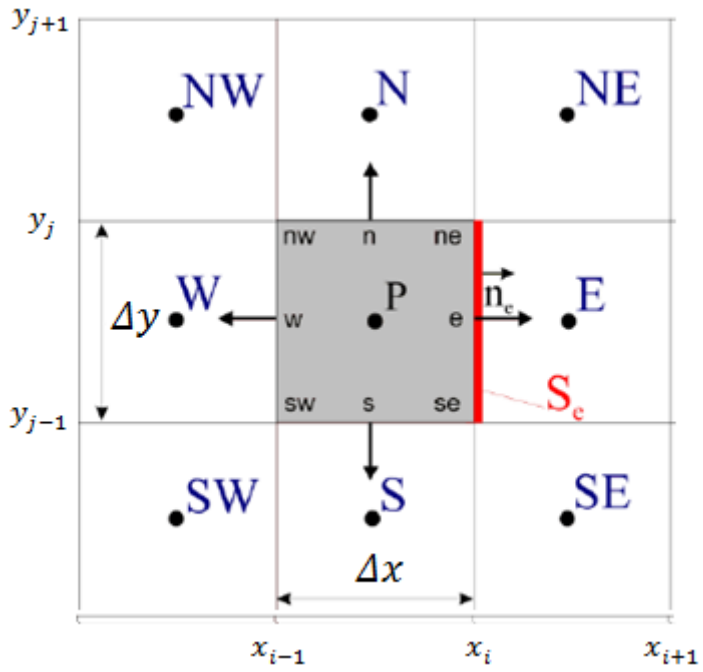

Figure 3.3: 2D example of vertex-centered FVM.

For this method, we continue with the integral form of general conservation equation

$$\frac{\partial}{\partial t}\iiint_V \rho\phi\, dV + \oiint_S \rho\vec{u}.\vec{n}dS = \iiint_V \vec{q}\, dV \tag{2.30}$$

For the unsteady-state systems, the time term is evaluated by simple integration over time

$$\int_{t_n}^{t_{n+1}} \frac{\partial \rho\phi S}{\partial t} dt = \phi(\rho^{n+1}S^{n+1} - \rho^n S^n) \tag{3.9}$$

The values at new timestep depend on the linearization scheme described in section 3.3.

The net flux through each surface of CV is the sum of the integrals over faces

$$\oiint_S \rho\vec{u}.\vec{n}dS = \sum_k \oiint_{S_k} \rho\vec{u}dS \tag{3.10}$$

which can be approximated by different rules. For instance, midpoint rule considers the flux through the face $ne - se$ is equal to the flux of e

$$\oiint_{S_{ne-se}} \rho\vec{u}dS \approx (\rho\vec{u})_e . S_{ne-se} \tag{3.11}$$

Trapezoidal and Simpsons rule are the other rules for approximation the surface integrals with more detailed information of the fluxes at the faces. Interpolation can be applied if the values of fluxes are unknown.

The source term of equation (2.30) can be approximated simply by

$$\iiint_V \vec{q}\, dV \approx \vec{q}_P V_{CV} \tag{3.12}$$

where V_{CV} is the volume of the control volume.

This is a fairly accurate approximation for variable q, but exact for constant or linear q.

3.3 Linearization Schemes

After discretization of the PDEs, the nonlinear coupling should be treated. In this section we will review the linearization methods most commonly used in reservoir simulation. The application of three types of methods in reservoir engineering will be discussed: Fully Implicit (FI), IMplicit Pressure - Explicit Saturation (IMPES), and Adaptive Implicit Method (AIM). Theoretically, the FI method is unconditionally stable and therefore, more implicit feature in the solution scheme is leading to more stable results.

3.3.1 Fully Implicit (FI)

In fully implicit method, the values at current time, $n+1$, are computed from the unknown values at the same time which requires more computational effort, i.e., in the case of flow equation in porous media, pressure and saturation are both calculated simultaneously. This results in an increased number of iterations per timestep which consequently raises the computational cost of the simulation. Nevertheless, this method assures most credible results.

The following equation shows the approximation of $(\rho S)^{n+1}$ in equation (3.9) when FI method is applied

$$(\rho S)^{n+1} = (\rho S)^n + f(t_{n+1}, (\rho S)^{n+1}).\Delta t \tag{3.13}$$

3.3.2 Implicit Pressure Explicit Saturation (IMPES)

The main idea behind IMPES method is to decouple the pressure and saturation equations. Namely, the pressure equation is solved implicitly while the saturation equation is updated explicitly. This decreases the computational error as the number of equations is half of the

one in FI. The time term of equation (2.30) presented in equation (3.9) can be approximated explicitly, after the pressure update, with

$$(\rho S)^{n+1} = (\rho S)^n + f(t_n, (\rho S)^n).\Delta t \tag{3.14}$$

where the pressure has been obtained implicitly previously.

Figure 3.4 (see [15]) illustrates a general flow chart showing the difference in the FI and IMPES methods. The simulation starts with reading the input data and initializing the reservoir. Afterwards, the primary unknowns and the coefficients in the flow equations are solved.

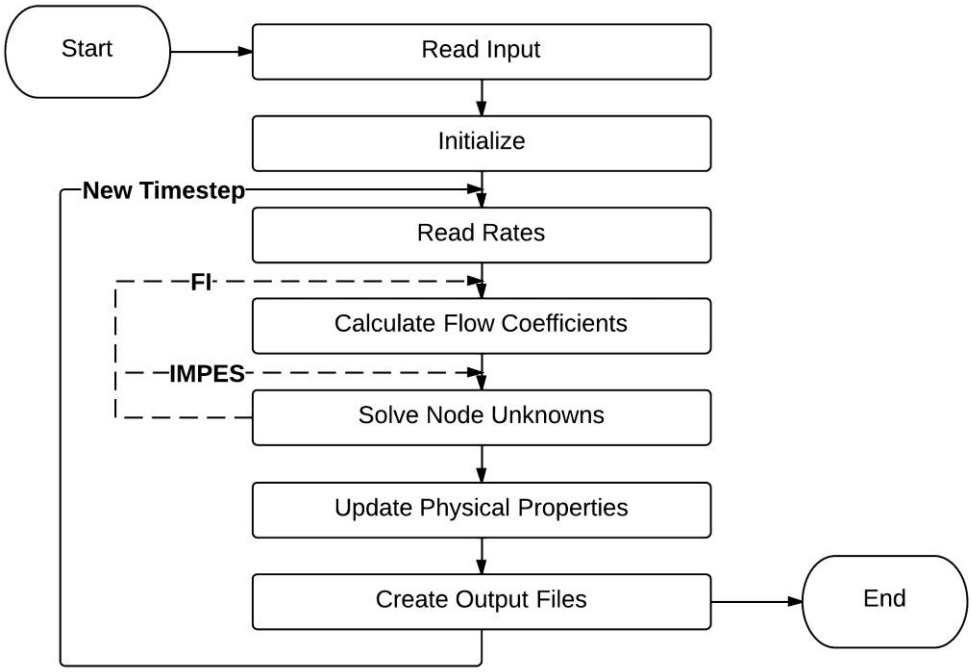

Figure 3.4: Typical flow chart in reservoir simulators showing FI and IMPES methods

The differences between two methods are in the calculations per timestep and updating the flow coefficients for solving the primary unknowns. In simulating the flow systems through porous media, FI methods do more iteration to solve for saturation and pressure at the same step, while IMPES requires less calculation effort.

3.3.3 Adaptive Implicit Method (AIM)

In 1983, Thomas and Thurnau [16] suggested the use of the Adaptive Implicit Method (AIM) which benefits a variable degree of implicitness. Its aim is to obtain saturation and pressure implicitly in the regions where courant number is larger than unity or there exists large variations in the saturations. In the other regions of the reservoir only the pressure is considered implicitly. This helps in saving the computational effort and cost. The main difficulty exists in AIM is the shifting criterion to change the procedure to FI and vice-versa. The efficiency of shifting criterion basically defines the success of AIM implementation. More details can be found in the above-mentioned reference.

.

Part II

Analysis

4 Methods

The program code in Brilliant is object orientated and written in C++. It is developed based on the conservation equation for each mass to calculate the pressure and saturation fields. In this work, the already implemented numerical method, FVM, has been modified for two phase flow. First the transmissibilities in the FVM code have been corrected. The convective term summed over the two phases' convective term. Capillary pressure equations and different relative permeability models have also been added to the code.

This section discusses the implementation methods used for numerically representing the multiphase flow through porous media. Due to the limiting time frame, the implementation was restricted to the two-phase flow of oil and water. The developed code is confidential, and therefore cannot be presented in the report. However, the details of the simulations have been given.

Calculating the differential equation for each phase should be taken into account. Capillary pressure together with the relative permeability of each phase controls the flow of the phases. These two parameters are nonlinearly dependent of the saturation of the phases. In order to implement multiphase flow in the code, the following assumptions have been made:

- The first phase is the wetting phase
- Phases are immiscible
- No phase change occurs

To start the implementation, a simplified model with some made up data has been used for debugging the code with Eclipse. After verification of the model, some SPE cases were simulated with Brilliant.

4.1 Pressure-Saturation Formulation of Two-Phase Flow

As it is described in chapter 2, it is required to solve two partial differential equations together with two constraint equations for obtaining the four unknowns in the multiphase flow model. The constraint equations are used for elimination of two unknowns. In this work, the equations are posed in terms of water phase saturation and oil phase pressure in pressure-saturation formulation. The other two unknowns, water phase pressure and oil phase saturation can then be obtained easily via the algebraic constraint equations of capillary pressure and saturation.

By exploiting the saturation constraint equation, equation (2.13), the PDEs can be restated as functions of two primary unknowns, p_o and S_w. After Substituting

$$S_o = 1 - S_w \tag{4.1}$$

and

$$p_w = p_o - \ p_c(S_w) \tag{4.2}$$

equations (2.38) and (2.39) reduce to

$$\frac{\partial(\rho_w \phi S_w)}{\partial t} - \overline{\overline{\nabla}}.\left(\rho_w \frac{k k_{rw}}{\mu_w}(\overline{\overline{\nabla}}\, p_o - \overline{\overline{\nabla}}\, p_c(S_w) - \rho_w g\, \overline{\overline{\nabla}}\, z)\right) = q_w \tag{4.3}$$

$$\frac{\partial(\rho_o \phi(1 - S_w))}{\partial t} - \overline{\overline{\nabla}}.\left(\rho_o \frac{k k_{ro}}{\mu_o}(\overline{\overline{\nabla}}\, p_o - \rho_o g\, \overline{\overline{\nabla}}\, z)\right) = q_o \tag{4.4}$$

Considering compressible fluid flow, the time derivatives in the PDEs of each phase can be expanded as follows

$$\left\{\rho_\alpha S_\alpha \frac{\partial \phi}{\partial t} + \phi S_\alpha \frac{\partial \rho_\alpha}{\partial t} + \phi \rho_\alpha \frac{\partial S_\alpha}{\partial t}\right\} - \overline{\overline{\nabla}}.\left(\rho_\alpha \frac{k k_{r\alpha}}{\mu_\alpha}(\overline{\overline{\nabla}}\, p_\alpha - \rho_\alpha g\, \overline{\overline{\nabla}}\, z)\right) = q_\alpha \tag{4.5}$$

Using chain rule, time derivate of phase density can be expressed as pressure derivative and the definition of the compressibility can then be applied in the equations.

4.1.1 Pressure Equation

In order to obtain the pressure equation, the mass conservation equation is summed over the phases. The time derivative term is expanded as stated in equation (4.5). To eliminate the phase saturations time derivative terms, PDEs are divided by the phase densities, giving the general form of

$$\frac{\partial \phi}{\partial t} - \sum_{\alpha=1}^{N_p} \overline{\overline{\nabla}}.\left(k \lambda_\alpha(\overline{\overline{\nabla}}\, p_\alpha - \rho_\alpha g\, \overline{\overline{\nabla}}\, z)\right) + \sum_{\alpha=1}^{N_p} \frac{1}{\rho_\alpha}\left[\phi S_\alpha \frac{\partial \rho_\alpha}{\partial t} + u_\alpha.\overline{\overline{\nabla}}\, \rho_\alpha\right] - \sum_{\alpha=1}^{Np} \frac{q_\alpha}{\rho_\alpha} = 0 \tag{4.6}$$

where Np is the number phases.

For the system of multiphase consisting only water and oil, equation (4.6) in terms of primary variable reduces to

$$\begin{aligned}\frac{\partial \phi}{\partial t} - \overline{\overline{\nabla}}.\, k &\left(\lambda_o\, \overline{\overline{\nabla}}\, p_o - \lambda_w \frac{\partial p_{cow}}{\partial S_w}\, \overline{\overline{\nabla}}\, S_w - (\lambda_w \rho_w - \lambda_o \rho_o) g\, \overline{\overline{\nabla}}\, z\right) \\ &+ \left(\frac{1}{\rho_w}\left[\phi S_w \frac{\partial \rho_w}{\partial t} + u_w.\overline{\overline{\nabla}}\, \rho_w\right] + \frac{1}{\rho_o}\left[\phi(1 - S_w)\frac{\partial \rho_o}{\partial t} + u_o.\overline{\overline{\nabla}}\, \rho_o\right]\right) = \frac{q_w}{\rho_w} + \frac{q_o}{\rho_o}\end{aligned} \tag{4.7}$$

where p_{cow} is the capillary pressure, and because it is a function of S_w, its derivative is written with respect to water phase saturation using chain rule. The density can be expressed in terms of compressibility c_o and c_w.

The solution of equation (4.7) gives the oil phase pressure. The water phase pressure can be obtained via equation (2.15)

$$p_w = p_o - \ p_{cow}(S_w) \tag{2.15}$$

4.1.2 Saturation Equation

Saturation equation exploits the Darcy velocity obtained from the pressure. The saturation equations are written per phase. In the system of multiphase the saturations are solved for $(Np-1)$ phases and the saturation of the last phase is calculated via constraint equation. The general form of the saturation equation is

$$\frac{\partial(\rho_\alpha \phi S_\alpha)}{\partial t} - \overline{\overline{\nabla}}.\left(\rho_\alpha k \lambda_\alpha (\overline{\overline{\nabla}}\, p_\alpha - \rho_\alpha g\, \overline{\overline{\nabla}}\, z)\right) = q_\alpha \tag{4.8}$$

In this thesis, for the specific case of water-oil flow, the saturation equation is written for the water phase

$$\frac{\partial(\rho_w \phi S_w)}{\partial t} - \overline{\overline{\nabla}}.\left(\rho_w k \left(\lambda_w\, \overline{\overline{\nabla}}\, p_o - \lambda_w \frac{\partial p_{cow}}{\partial S_w}\, \overline{\overline{\nabla}}\, S_w - \lambda_w \rho_w g\, \overline{\overline{\nabla}}\, z\right)\right) = q_w \tag{4.9}$$

and the oil phase saturation is calculated by equation (4.1)

$$S_o = 1 - \ S_w \tag{4.1}$$

4.2 Numerical Model

Brilliant uses FVM to decouple the PDEs. For the system of multiphase this method is applied for the multiphase by adding the concept of relative permeability and capillary pressure. The transmissibility term which contains the mobility term is revised. After decoupling, the equations are linearized by IMPES method. This section summarizes the numerical model applied for simulating the multiphase flow.

4.2.1 Decoupling PDEs - Finite Volume Method

FVM is employed for discretization of the numerical formulation of equations (4.7) and (4.9). Considering Fig. 4.1, where the gray cube in Fig. 3.3 is shown in more detail in 3D, the discrete form of the pressure equation is as follows

$$T_P^n p_P^{n+1} = T_E^n p_E^{n+1} + T_W^n p_W^{n+1} + T_N^n p_N^{n+1} + T_S^n p_S^{n+1} + T_F^n p_F^{n+1} + T_B^n p_B^{n+1} + f_P^n \tag{4.10}$$

where the coefficients T are the transmissibilities of each CV in the form of equation (3.2). The subscripts indicate the node and the superscripts n and $n+1$ show the old and current time, respectively. The details of the coefficients can be found in Appendix A.

The discrete saturation equation is written in the same manner

$$\begin{aligned} S_P^{n+1} = {} & S_P^n + a_P^n S_P^n - (a_E^n S_E^n + a_W^n S_W^n + a_N^n S_N^n + a_S^n S_S^n + a_F^n S_F^n + a_B^n S_B^n) \\ & - c_P^n p_P^n + (c_E^n p_E^n + c_W^n p_W^n + c_N^n p_N^n + c_S^n p_S^n + c_F^n p_F^n + c_B^n p_B^n) \\ & + d_P^n z_P^n - (d_E^n z_E^n + d_W^n z_W^n + d_N^n z_N^n + d_S^n z_S^n + d_F^n z_F^n + d_B^n z_B^n) + \overline{\left(\frac{q_w}{\rho_w}\right)}\Big|_P \frac{\Delta t}{\phi} \end{aligned} \tag{4.11}$$

The coefficients are to be found in Appendix A.

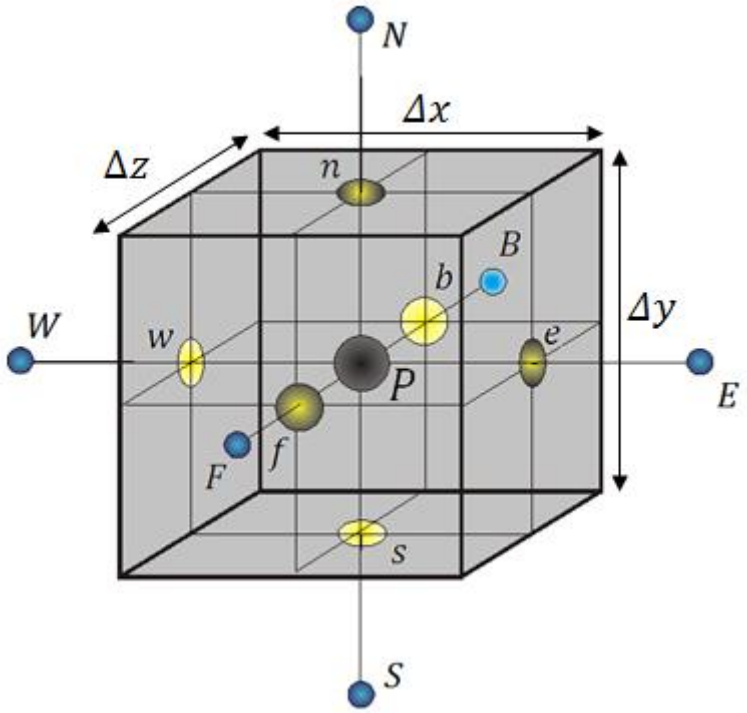

Figure 4.1: The Finite difference method. The center of the volumes are labeled with uppercase letters, meanwhile the faces are labeled using lowercase letters.

4.2.2 Linearizing Discretized PDEs – IMPES Method

In the code developed in Brilliant, the solver uses the so-called IMPES method as the linearizing scheme. Fig. 4.2 illustrates the flow chart of the implemented algorithm. After reading the input data, it first solves for the pressures of the phases implicitly. Moreover, it obtains the phase saturations explicitly. Afterwards, if the solution converges, it continues to the next timestep. Otherwise, more iteration needs to be done for reaching the convergence. The maximum number of iterations was set to 14. If the solution could not converge after 14 iterations, the simulation crashed.

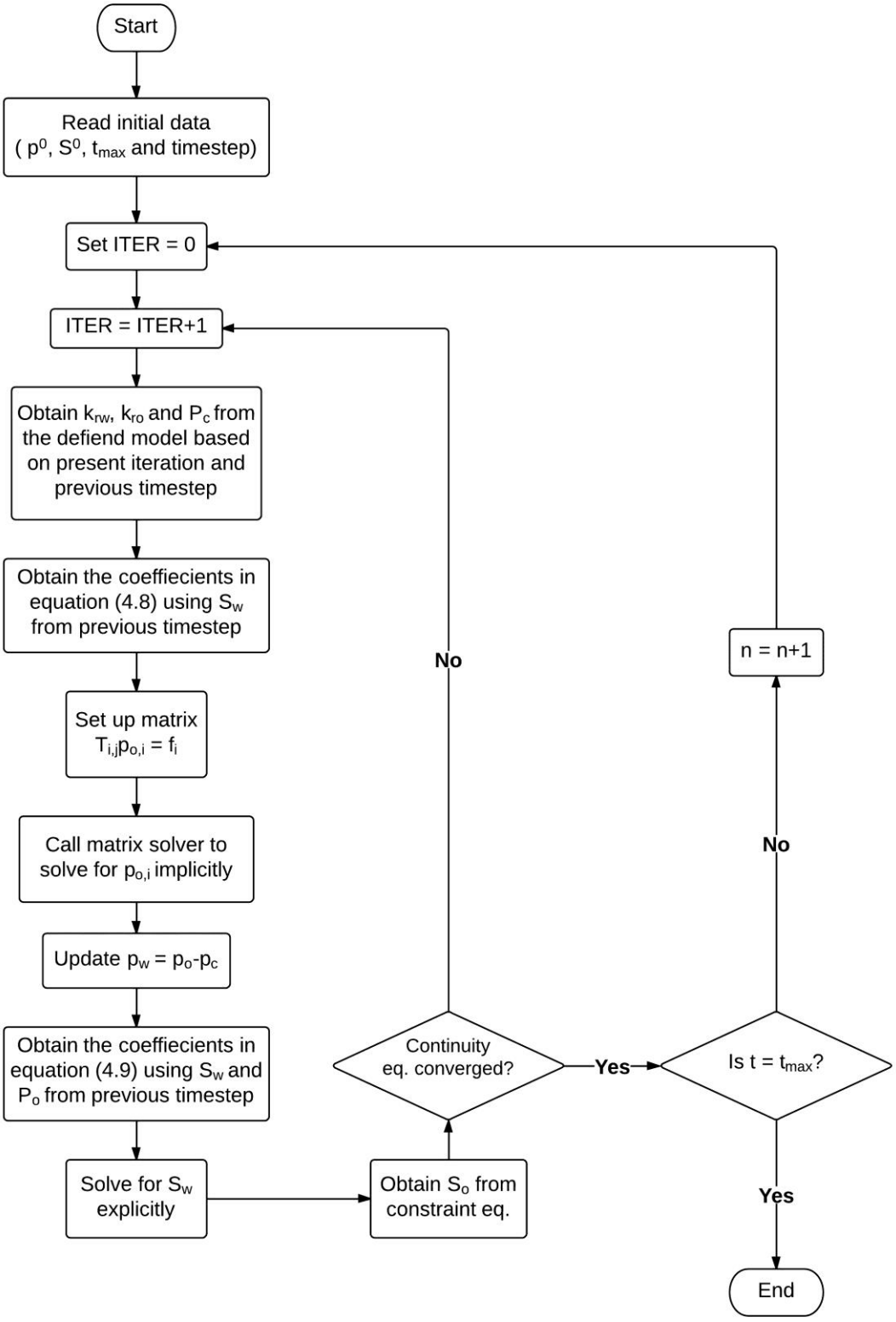

Figure 4.2: Flow chart of the IMPES method implemented in the code

4.2.3 Mobility Selection

As it has been discussed in Subs. 3.1.3, the upstream mobility selection is more stable and accurate than the other methods. Therefore, the mobility in the faces of the CV is defined as

$$\lambda_{\alpha_{i+\frac{1}{2}}} = \begin{cases} \lambda_{\alpha_{i+1}} & if \quad p_{\alpha_{i+1}} \geq p_{\alpha_i} \\ \lambda_{\alpha_i} & if \quad p_{\alpha_{i+1}} < p_{\alpha_i} \end{cases} \tag{4.12}$$

As an example, Fig. 4.3 shows the mobility selection for the face e.

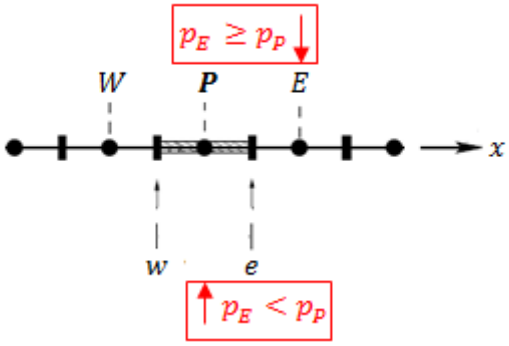

Figure 4.3: Mobility selection for face *e*

4.2.4 Relative Permeability Model

The existence of more than one fluid phase in a CV means that the flow behavior of the phases is disturbed by each other. The aim of this part is to examine the effect of different relative permeability models on the simulation results. The code has been compiled by defining three types of relperm correlations: (1) the correlated data from SPE cases for testing the code. (2) Corey's Two-Phase Relative Permeability Model, (3) Naar and Henderson's Two-Phase Model.

For the definition of the models, the reader is referred to section 2.4.

4.2.5 Capillary Pressure Model

The capillary pressure model is an essential prerequisite model for the simulation of multiphase in porous media. In this thesis, because of the lack of data for the parameters in the empirical correlations, the simulations are done with correlating the capillary pressure data based on the wetting phase saturation from different SPE cases.

5 Numerical Results

This chapter presents the numerical results achieved from Brilliant and Eclipse. With the aim of testing the implemented multiphase model in the code, a self-constructed test case in addition to one SPE case was run in both Brilliant and Eclipse to carry out a comparison between two simulators. Afterwards, some simulations were run in Brilliant to see what effect the different relative permeability models have on the simulation results.

The tests are done according to the descriptions provided in the previous chapter.

It is worth to mention that the presented simulation cases are not the only ones done in Brilliant, and only a number of those simulations are mentioned in this chapter.

5.1 Test Cases

This section provides the results of the test case simulations in Eclipse and Brilliant performed for validating the implemented multiphase model.

5.1.1 First Test Case: Self-Constructed Case

Prior to benchmarking the code with a SPE case, a test case was made aiming to verify the physical phenomena applied for the water-oil system in the code.

Model description. In this case, we consider a porous media whose geometry is shown in Fig. 5.1.Here we use a 10×7×6 grid, in which each grid block has the dimensions of 5×5×5 m^3. Yellow and blue CVs show the well perforations.

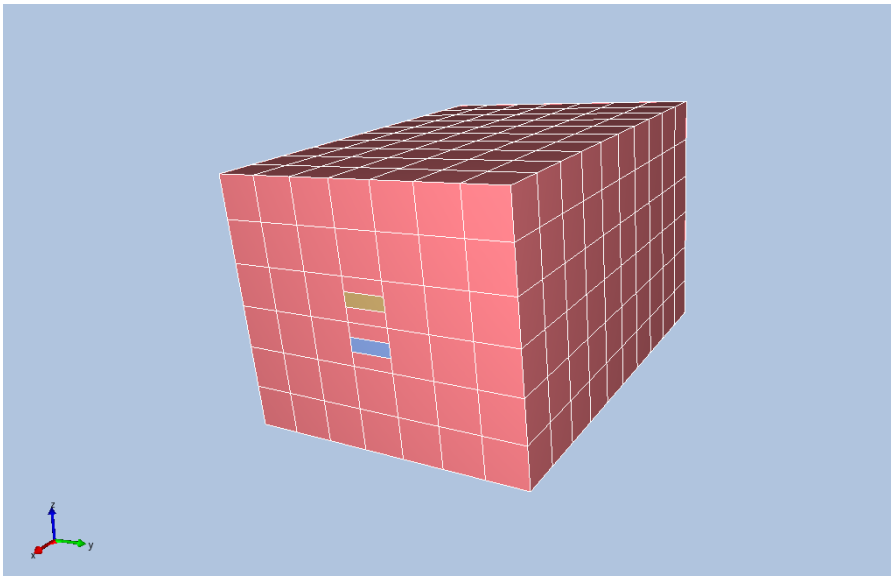

Figure 5.1: 3D visualization of the self-constructed test case

A production well is located at the right side (10, j, k) of the system, producing with bottomhole pressure boundary condition. The perforations are placed at the coordinates of (10, 4, 3) and (10, 4, 4). We advance the simulations to 100 days, with starting timestep of 0.001 days growing to 0.01 days.

The physical and geometrical data are listed in Tab. 5.1.

Table 5.1: Geometry data of the Self-constructed case

Reservoir Data	Initial Conditions
$k_x = k_y = 1$ [md] $k_z = 0.1$ [md]	$S_{wi} = 0.20$
h = 30 [m]	$p_i = 140$ [bars]
A = 35×50 [m^2]	$T_i = 340.15$ [K]
$\phi = 0.5$	
Top = -3535 [m]	

The porous media consists of water and oil phases where the oil phase is specified to contain only i-C_6. Oil phase is not allowed to dissolve in the water phase, and water is not present in the oil phase. This is the case that we called pseudo-compositional in chapter 2, where black-oil simulator can be used to simulate the multicomponent-multiphase system with only one component in the hydrocarbon phase.

All the thermodynamics properties, such as speed of sound for the compressibility of both phases, are obtained based on Peng-Robinson equation of state (PR-EOS)[17]

$$p = \frac{RT}{V_m - b} - \frac{a}{V_m(V_m + b) + b(V_m - b)} \tag{5.1}$$

where

$$b = 0.07780 \frac{RT_c}{p_c} \tag{5.2}$$

$$a = 0.45724 \frac{(RT_c)^2}{p_c} \left[1 + m\left(1 - \sqrt{T_r}\right)\right]^2 \tag{5.3}$$

and

$$m = 0.37464 + 1.54226\omega - 0.26992\omega^2 \tag{5.4}$$

ω is the acentric factor for the components. p_c and T_c are the critical properties of the components. V_m is the molar volume, and R indicates the universal constant. Pseudo-reduced temperature T_r is equal to $\frac{T}{T_c}$.

Tab. 5.2 shows the component properties used in the PR-EOS within Brilliant.

Table 5.2: Fluid critical properties used in PR-EOS in Brilliant

	M_{w_i} [kg/kgmol]	T_{c_i} [K]	p_{c_i} [bars]	ω_i
i-C_6	86.18	497.5	30.10	0.278
Water	18.02	647.14	220.50	0.329

The $p_c - S_w$ and relperm curves are, respectively, illustrated in Fig. 5.2 and 5.3.

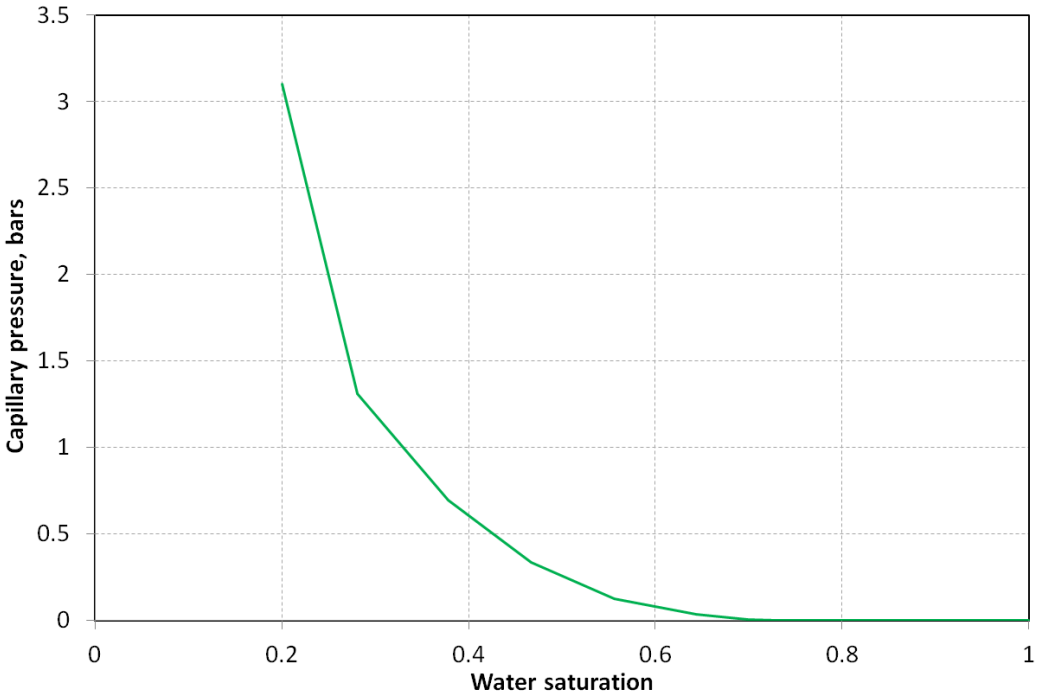

Figure 5.2: Capillary pressure-water saturation curve for self-constructed case

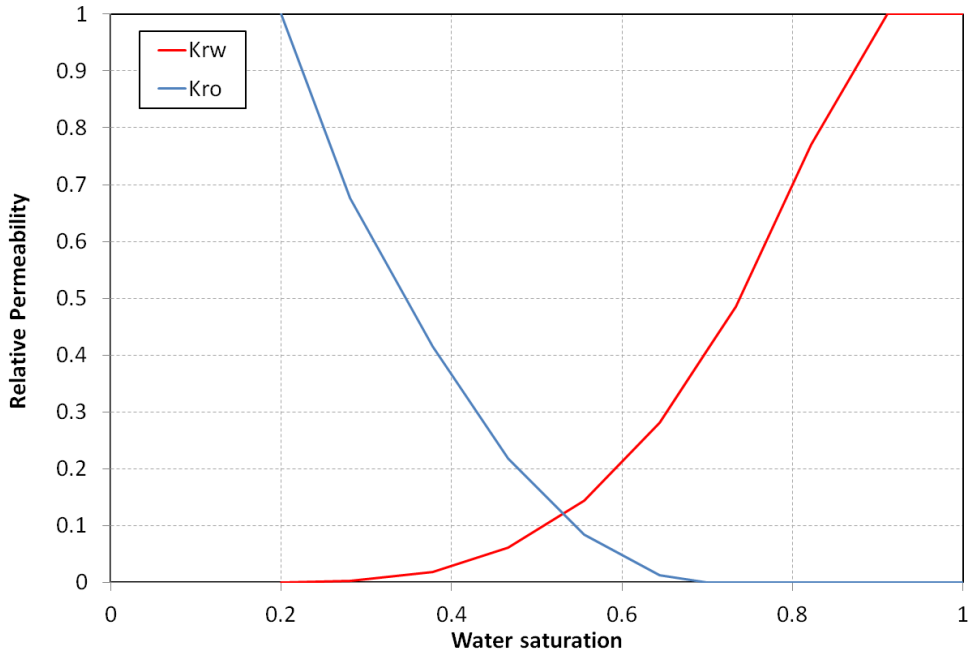

Figure 5.3: Oil phase (blue) and water phase (red) relperm curves

Pressure boundary conditions are chosen as the production scenario of the oil phase. The pressure in both the upper and lower perforations are set to be decreasing in the same trend, but because of the gravity effect the lower boundary will definitely have a little bit more pressure decline than the other.

The script file of the Eclipse model for the self-constructed case is presented in Appendix B-1.

Simulation Results. The pressure profiles for two simulators are illustrated in Fig. 5.4.

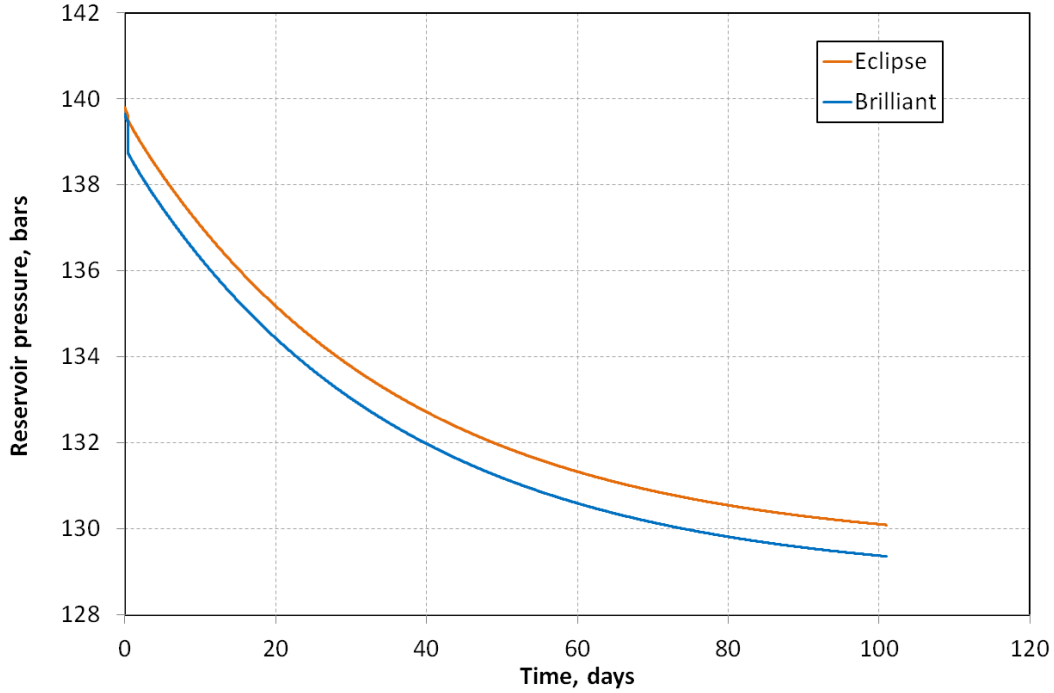

Figure 5.4: Comparison of pressure profile, self-constructed case

5.1.2 Second Test Case: Five Spot Model

A SPE case is used for further testing of the multiphase model. Existing models in Brilliant use Navier-Stokes equation for modeling the flow. Up to now, no convenient model has been implemented for modeling multiphase flow with high fraction of liquid inside a tubing/well. Although problem of not having a multiphase flow model for the well could be prohibited in production scenarios, it was not possible to add injection well to the model. Therefore, the injection well in this case is removed.

Model description. This case models a homogeneous, isotropic 5x5x1 quarter five spot. The geometry of the case is shown in Fig. 5.4.

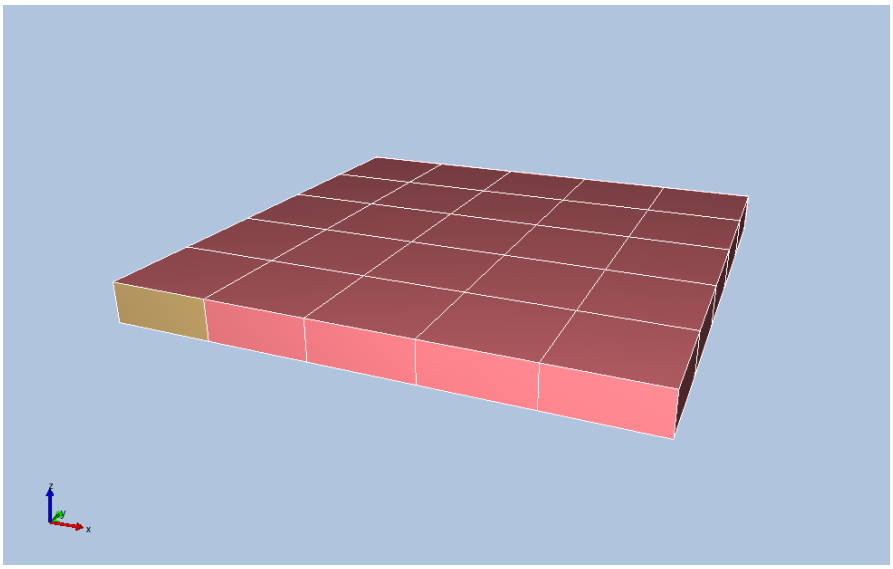

Figure 5.4: 3D visualization of the SPE test case

A production well is located at the right side (5, 5, 1) of the system, producing with bottomhole pressure boundary condition. Since this is a medium with only one-layer in z-direction, there was only one perforation for the production well. The simulation was performed for 100 days with the maximum timestep of 0.01.

The physical and geometrical data are listed in Tab. 5.1.

Table 5.3: Geometry data of the SPE test case

Reservoir Data	Initial Conditions
$k_x = k_y = k_z = 50$ [md]	$S_{wi} = 0.25$
h = 30 [m]	$p_i = 275$ [bars]
A = 375×375 [m^2]	
$\phi = 0.2$	
Top = -4000 [m]	

The same as the previous test case, the thermodynamics properties for Brilliant, are calculated via PR-EOS.

Relative permeabilities and capillary pressure are chosen to be varying linearly with respect to water saturation for this case. Figures 5.5 and 5.6 demonstrate the $p_c - S_w$ and relperm models for this case.

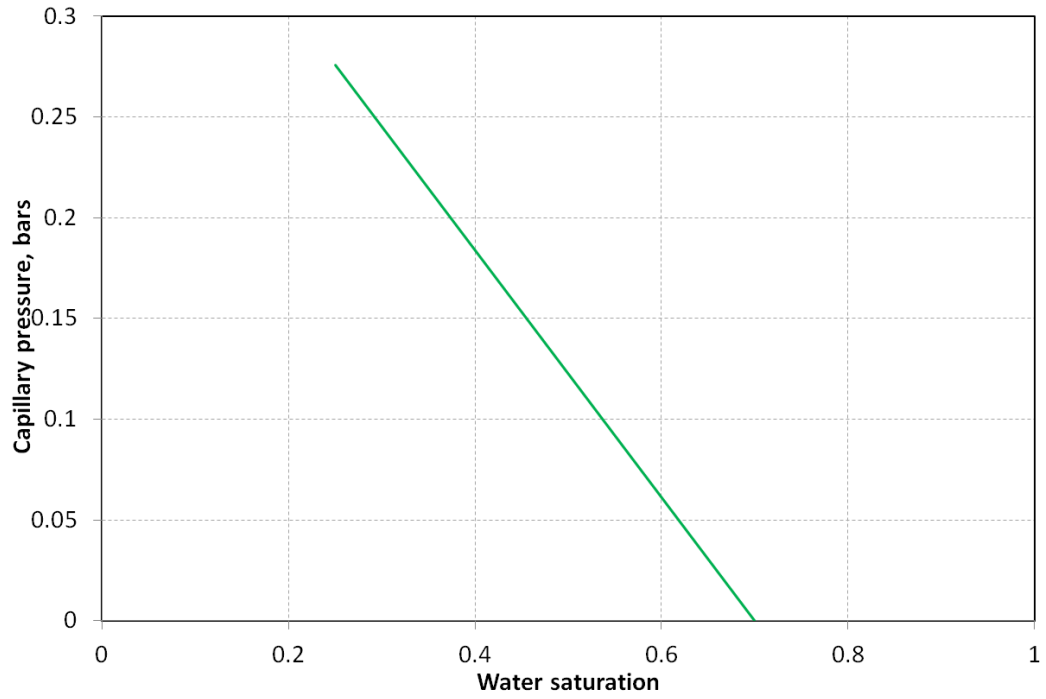

Figure 5.2: Capillary pressure-water saturation curve for self-constructed case

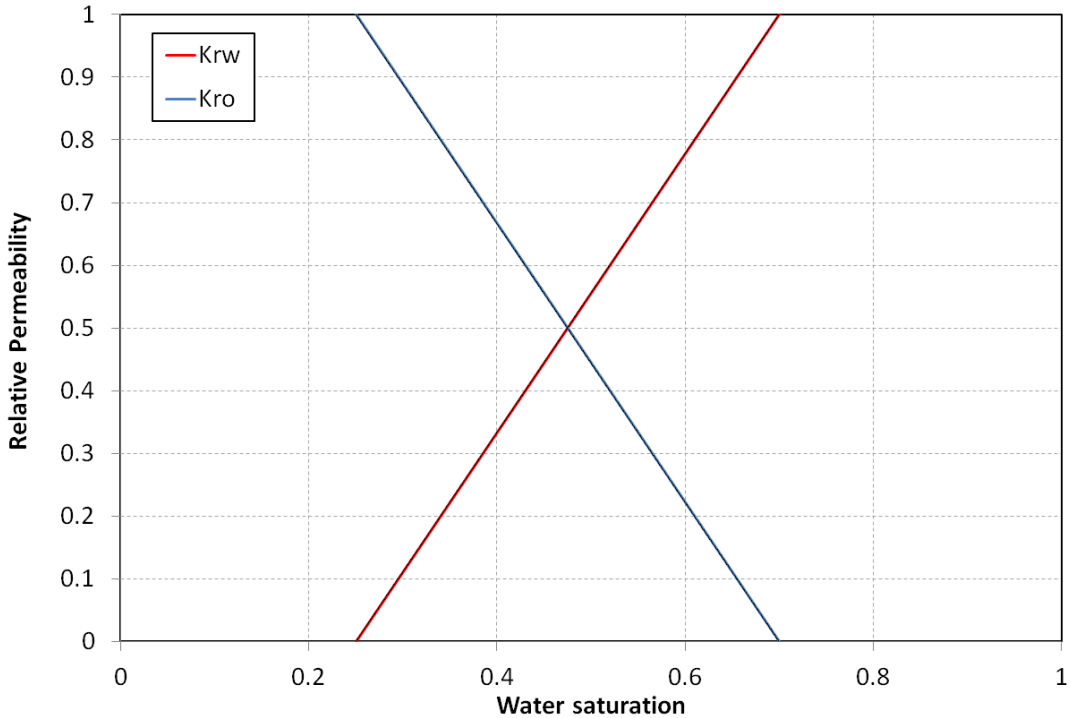

Figure 5.6: Oil phase (blue) and water phase (red) relperm curves

The fluid is produced with the constraint of minimum bottomhole pressure. The script file of the Eclipse model for the self-constructed case is presented in Appendix B-2.

Simulation Results. The results for this case showed a significant difference between two simulators. This is obviously because of the wrong density calculation in Brilliant, since the density in the Eclipse model is not assigned based on the average value from PR-EOS calculation. Fig. 5.7 presents the performance of two simulators for 100 days of simulation time.

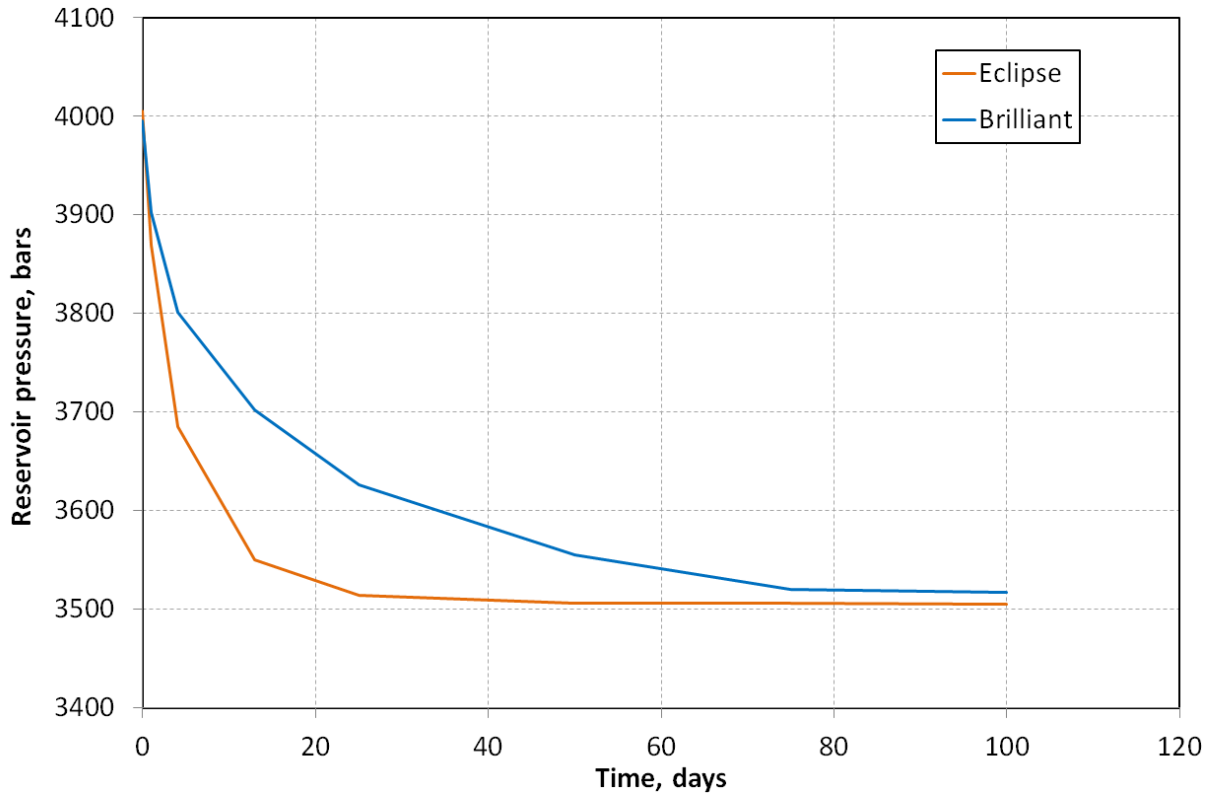

Figure 5.7: Comparison of pressure profile, self-constructed case

5.2 Simulation with Different RelPerm Correlations

After benchmarking, the code has been compiled with different relperm correlations. For this thesis, Corey's two-phase relperm correlation is compared with Naar and Hendersons' correlation. These two formulations use identical $k_{rw} - S_w$ relationship. The differences arise from the oil phase relative permeability correlation. The details of the correlations are defined in section 2.4.

For the aim of comparing the relperm correlations, the same system as the self-constructed case is used.

Fig. 5.7 compares the pressure profile for two relperm formulations.

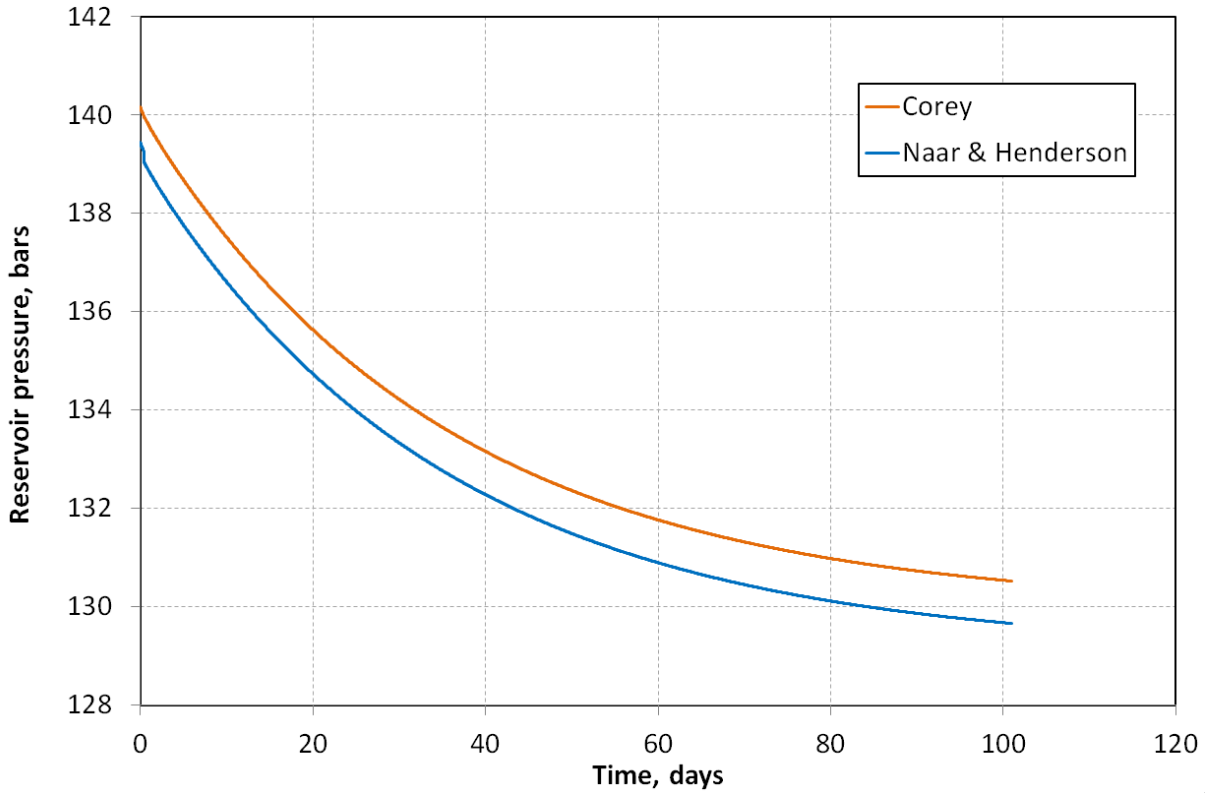

Figure 5.7: Reservoir pressure profile for two relperm formulations

Two formulations showed almost identical results in the further analysis of the outputs. Therefore, only the analysis of simulation with Corey's relperm model is reported.

Fig. 5.8 shows the pressure profile along the reservoir at various simulation times from beginning to end.

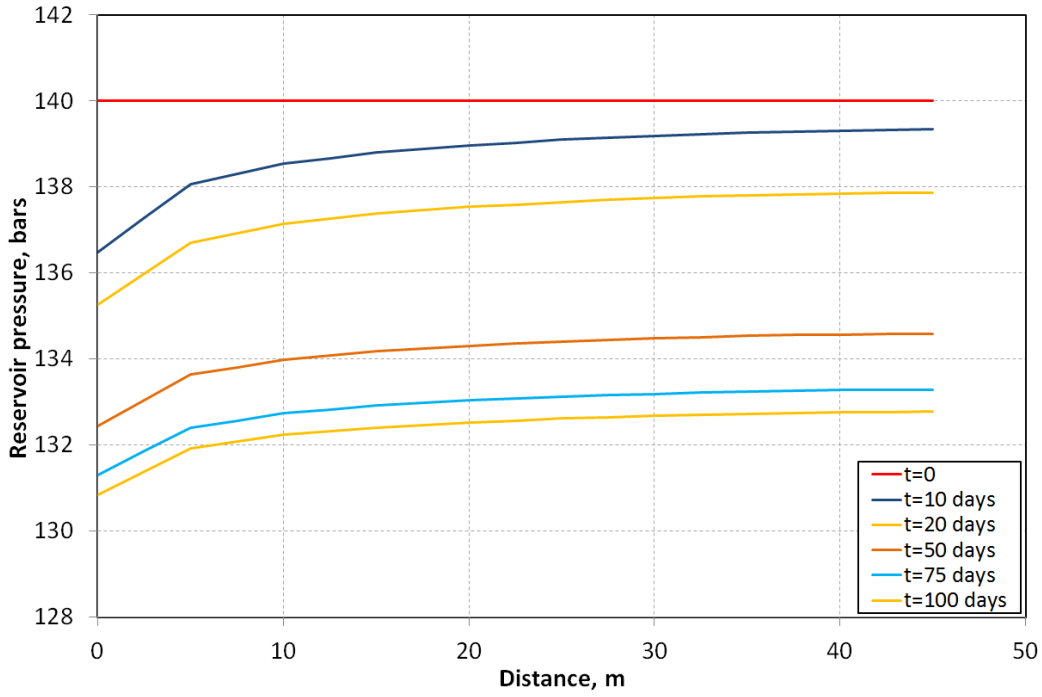

Figure 5.8: Reservoir pressure profile with respect to distance

Fig. 5.9 shows the state of system for different steps of simulation represented by reservoir pressure.

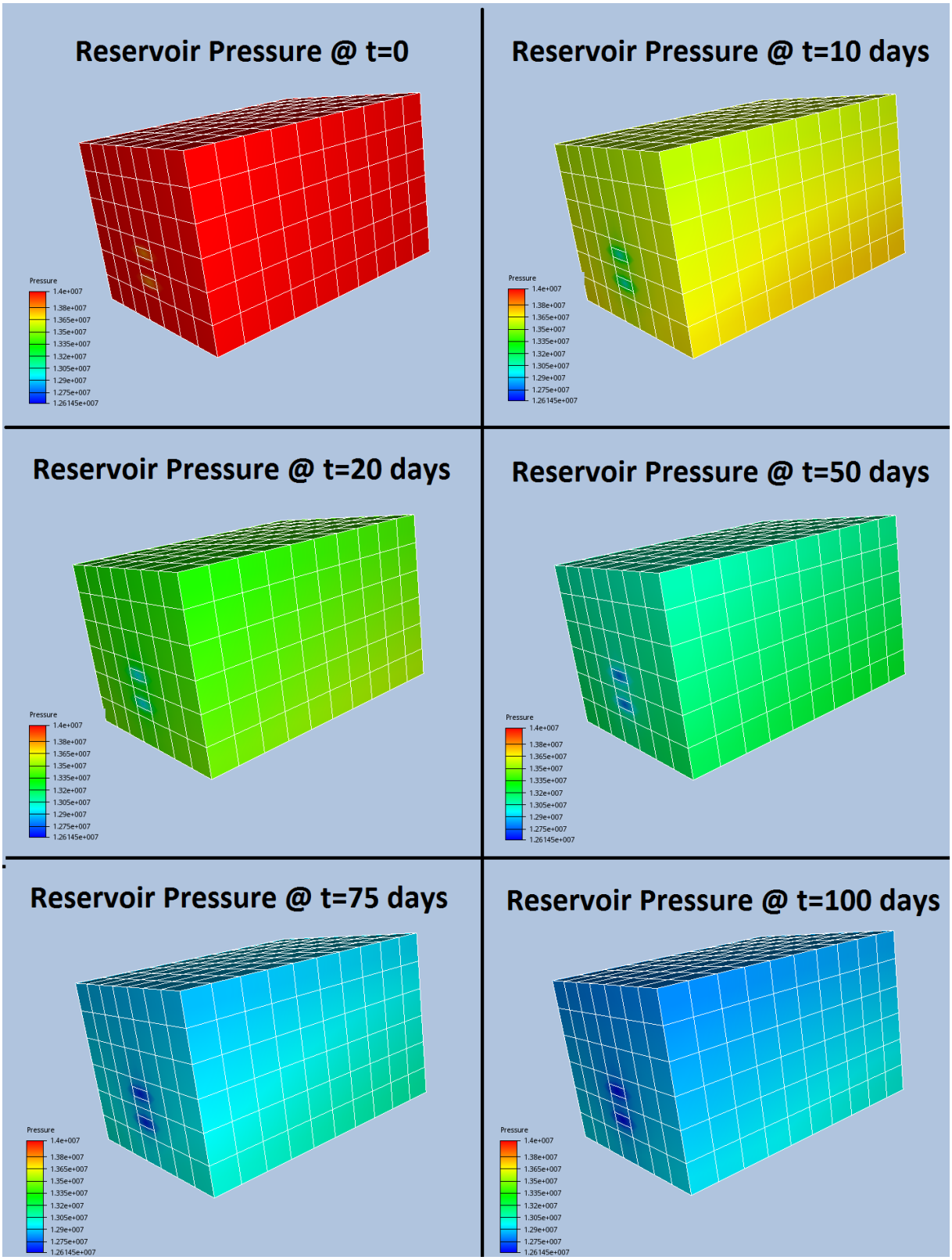

Figure 5.9: State of reservoir in terms of pressure

Part III

Summary

6 Discussions

In the following, the results of the simulations with the implemented multiphase model are discussed. This chapter also provides some thoughts about the future work on the multiphase flow model in Brilliant.

6.1 Simulation Results

In this thesis, multiphase flow is simulated first for testing the implemented code, and then for estimating how accurate various relperm models perform in prediction of the flow of fluids in the presence of the other fluids. This section discusses the results of the performed simulations.

6.1.1 Self-Constructed Test Case

As Brilliant uses a compositional system for simulation, the consistency in its simulation results with the ones from Eclipse, can be a confirmation of the statement presented in chapter 2 that a black-oil simulator is a pseudo-compositional simulator when there is only one component the hydrocarbon phase.

6.1.2 SPE Case

This test had the same production scenario as the self-constructed test case. The only difference in performing the simulation is this was the tuning of the density. Although the pressure profiles for two simulators showed similar trend of pressure decline, but the difference between the performances was quite significant compared to the first case where the fluids were subject to the same density value.

6.2 Limitations and Challenges

The main challenge in running the simulations in Brilliant was related to thermodynamics. As the other CFD packages, EOS is used for calculating the PVT properties in Brilliant. This EOS should be tuned for all the flowing fluids to perform a flawless simulation. Brilliant is limited to use only one EOS for all the fluids in the system; therefore the general form of PR-EOS is used for obtaining the water properties which gave some values, such as density, far from the reality. In the self-constructed test case, the density values were chosen in a way that they have the average value calculated via PR-EOS, but this was not done for the five spot test case. This is one reason that the SPE test case end up with less accurate simulation outcome.

The lack of multiphase model for the tubing while the flowing phases have high liquid fraction limited the simulations to production cases, and accordingly no fluid could be injected to the reservoir. It was not possible to ignore the well as the way is done for the productions. This is

due to the fact that the pressures in FVM are calculated based on the neighboring CV. Thus, the neighboring CV existing in the tubing is necessary for calculation of pressure in boundary CV.

6.3 Future Work

In this thesis, only one case of multiphase flow has been implemented. There are definitely much to do to improve the code in all aspects, but with regard to the multiphase flow, the implemented code can be extended to two-phase flow of gas-oil, gas condensate reservoir and three-phase flow by including the mass transfer between phases, Rs in the general form of the flow equations in porous media presented in chapter 2.

7 Conclusions

This chapter contains a summary of conclusions and remarks made in the previous chapters.

As the first objective in this master thesis, We succeeded to add the model of multiphase flow to the code. This is done by including the capillary pressure and relative permeability of the phases in the flow equations. Finite Volume Method (FVM) was chosen to be maintained in code as the discretization method. The main reason for this choice was the greater scope of this method compared to the other methods presented in chapter 3. This helped to, theoretically, bring the problem representation closer to reality.

As the implemented coding uses IMPES method, there was limitation in choosing the big time steps, as the IMPES method is sensitive to stability criterion, the courant number. Therefore, the time step is chosen in a way that it went on without crash

The tests were realized for two phase flows of water and oil. When viewing the results however, it is important to acknowledge the limitations of the model and the assumptions made in performing the simulations.

Bibliography

[1] Petrell AS: *About Petrell, (website),* URL: http://petrell.no/about/, 2010

[2] Brilliant: *Brilliant-CFD, (website),* URL: http://www.brilliant-cfd.com/, 2010.

[3] Fanchi, J.R.: *Principles of Applied Reservoir Simulation*. Butterworth-Heinemann Gulf Professional Publishing, 2nd edn., Boston, 2001.

[4] Ertekin, T., Abou-Kassem, J.H., King, G.: *Basic Applied Reservoir Simulation*. SPE Textbook Series Vol. 7, Richardson, Texas, 2001.

[5] Dong, L. and Gudmundsson, J.S.: *Model for Sound Speed in Multiphase Mixtures.* 3rd Lerkendal Petroleum Engineering Workshop, Norwegian Institute of Technology, Trondheim, January 20-21, 1993.

[6] Corey, A.T.: *The interrelation between gas and oil relative permeabilities*. Producers Monthly 19 (November): 38–41, 1954.

[7] Pirson, S.J.: *Oil Reservoir Engineering*. McGraw-Hill, New York, 1958.

[8] Naar, J. and Henderson, J. H.: *An imbibition model - Its application to flow behavior and the prediction of oil recovery.* SPE J. 61-70 (June), 1961.

[9] Mohamed, I.M.N., and Koederitz, L.F.: *Two-Phase Relative Permeability Prediction Using a Linear Regression Model.* Morgantown, W.Va: Paper No. SPE 65631, SPE Eastern Regional Meeting, Oct. 17-19, 2000.

[10] Honarpour, M., Koederitz, L.F., and Herbert, A.H.: *Empirical Equations for Estimating Two-Phase Relative Permeability in Consolidated Rock*. JPT, pp. 2905-08, December 1982.

[11] Kleppe, J.: *Introduction to compositional simulation*. TPG4160-Reservoir Simulation Handout 14, Trondheim, 2013.

[12] Kleppe, J.: *Oil-water simulation-IMPES solution*. TPG4160-Reservoir Simulation Handout 6, Trondheim, 2013.

[13] Smith G.: *Numerical Solution of Partial Differential Equations: Finite Difference Methods*. Oxford University Press, 1985.

[14] Versteeg H. and Malalasekera W.: *An Introduction to Computational Fluid Dynamics*. The Finite Volume Method, Longman Scientific & Technical, 1995.

[15] Crichlow, H.B.: *Modern Reservoir Engineering - A Simulation Approach*. Englewood Cliffs, NJ: Prentice Hall, 1977.

[16] Thomas, G.W., Thurnau, D.H.: *Reservoir simulating using an adaptive implicit method*, SPEJ, Vol. 23, No. 5, pp. 759-768, 1983.

[17] Peng, D. Y., and Robinson, D. B.: *A New Two-Constant Equation of State*. Industrial and Engineering Chemistry: Fundamentals 15: 59–64, 1976.

Appendix A

The coefficients of equations (4.8) and (4.9) are presented in this appendix.

The coefficients of pressure equation are as follows

$$T_E^n = \frac{k_{11}\lambda_{o|_e}^n}{\Delta x_e} A_x; \qquad T_W^n = \frac{k_{11}\lambda_{o|_w}^n}{\Delta x_w} A_x;$$

$$T_N^n = \frac{k_{22}\lambda_{o|_n}^n}{\Delta y_n} A_y; \qquad T_S^n = \frac{k_{22}\lambda_{o|_s}^n}{\Delta y_s} A_y;$$

$$T_F^n = \frac{k_{33}\lambda_{o|_f}^n}{\Delta z_f} A_z; \qquad T_B^n = \frac{k_{33}\lambda_{o|_b}^n}{\Delta z_b} A_z; \qquad (A-1)$$

In the above transmissibility terms, Δx, Δy and Δz in the faces are defined as the sum of the face distance from the center of the neighboring CV in $x-$, $y-$ or $z-$direction.

If we define

$$T_e^n = \frac{k_{11}\lambda_{w|_e}^n}{\Delta x_e} A_x; \qquad T_w^n = \frac{k_{11}\lambda_{w|_w}^n}{\Delta x_w} A_x;$$

$$T_n^n = \frac{k_{22}\lambda_{w|_n}^n}{\Delta y_n} A_y; \qquad T_s^n = \frac{k_{22}\lambda_{w|_s}^n}{\Delta y_s} A_y;$$

$$T_f^n = \frac{k_{33}\lambda_{w|_f}^n}{\Delta z_f} A_z; \qquad T_b^n = \frac{k_{33}\lambda_{w|_b}^n}{\Delta z_b} A_z; \qquad (A-2)$$

and

$$b_e^n = \frac{(\rho_w\lambda_w^n - \rho_o\lambda_o^n)_{|_e}}{\Delta x_e}; \qquad b_w^n = \frac{(\rho_w\lambda_w^n - \rho_o\lambda_o^n)_{|_w}}{\Delta x_w};$$

$$b_n^n = \frac{(\rho_w\lambda_w^n - \rho_o\lambda_o^n)_{|_n}}{\Delta y_n}; \qquad b_s^n = \frac{(\rho_w\lambda_w^n - \rho_o\lambda_o^n)_{|_s}}{\Delta y_s};$$

$$b_f^n = \frac{(\rho_w\lambda_w^n - \rho_o\lambda_o^n)_{|_f}}{\Delta z_f}; \qquad b_e^n = \frac{(\rho_w\lambda_w^n - \rho_o\lambda_o^n)_{|_b}}{\Delta z_b}; \qquad (A-3)$$

Then we have

$$f_p^n = T_e^n \left(\frac{\partial p_{cow}^n}{\partial S}\right)_{|e} S_E^n + g b_e^n z_E + T_w^n \left(\frac{\partial p_{cow}^n}{\partial S}\right)_{|w} S_W^n + g b_w^n z_W$$
$$+T_n^n \left(\frac{\partial p_{cow}^n}{\partial S}\right)_{|n} S_N^n + g b_n^n z_N + T_s^n \left(\frac{\partial p_{cow}^n}{\partial S}\right)_{|s} S_S^n + g b_s^n z_S$$
$$+T_f^n \left(\frac{\partial p_{cow}^n}{\partial S}\right)_{|f} S_F^n + g b_f^n z_N + T_b^n \left(\frac{\partial p_{cow}^n}{\partial S}\right)_{|b} S_B^n + g b_b^n z_B$$
$$+ \left[\overline{(\frac{q_w}{\rho_w})} + \overline{(\frac{q_o}{\rho_o})} \right]_{|P} \Delta V \qquad (A-4)$$

The coefficients are written only for the incompressible system in this report. For the compressible system, the density changes are calculated in the same manner as saturation.

The coefficients of the saturation equation are given by

$$a_E^n = T_e^n \left(\frac{\partial p_{cow}^n}{\partial S}\right)_{|e} \frac{\Delta t}{\phi \Delta V}; \qquad a_W^n = T_w^n \left(\frac{\partial p_{cow}^n}{\partial S}\right)_{|w} \frac{\Delta t}{\phi \Delta V};$$
$$a_N^n = T_n^n \left(\frac{\partial p_{cow}^n}{\partial S}\right)_{|n} \frac{\Delta t}{\phi \Delta V}; \qquad a_S^n = T_s^n \left(\frac{\partial p_{cow}^n}{\partial S}\right)_{|s} \frac{\Delta t}{\phi \Delta V};$$
$$a_F^n = T_f^n \left(\frac{\partial p_{cow}^n}{\partial S}\right)_{|f} \frac{\Delta t}{\phi \Delta V}; \qquad a_B^n = T_b^n \left(\frac{\partial p_{cow}^n}{\partial S}\right)_{|b} \frac{\Delta t}{\phi \Delta V}; \qquad (A-5)$$

$$a_P^n = a_E^n + a_W^n + a_N^n + a_S^n + a_F^n + a_B^n \qquad (A-6)$$

and,

$$c_E^n = \frac{k_{11} \lambda_{w|_e}^n}{\Delta x_e} A_x \frac{\Delta t}{\phi \Delta V}; \qquad c_W^n = \frac{k_{11} \lambda_{w|_w}^n}{\Delta x_w} A_x \frac{\Delta t}{\phi \Delta V};$$
$$c_N^n = \frac{k_{22} \lambda_{w|_n}^n}{\Delta y_n} A_y \frac{\Delta t}{\phi \Delta V}; \qquad c_S^n = \frac{k_{22} \lambda_{w|_s}^n}{\Delta y_s} A_y \frac{\Delta t}{\phi \Delta V};$$
$$c_F^n = \frac{k_{33} \lambda_{w|_f}^n}{\Delta z_f} A_z \frac{\Delta t}{\phi \Delta V}; \qquad c_B^n = \frac{k_{33} \lambda_{w|_b}^n}{\Delta z_b} A_z \frac{\Delta t}{\phi \Delta V}; \qquad (A-7)$$

$$c_P^n = c_E^n + c_W^n + c_N^n + c_S^n + c_F^n + c_B^n \qquad (A-8)$$

Finally,

$$d_E^n = \frac{k_{11}\lambda_{w|_e}^n}{\Delta x_e}\rho_w g\frac{\Delta t}{\phi \Delta V}; \qquad d_W^n = \frac{k_{11}\lambda_{w|_w}^n}{\Delta x_w}\rho_w g\frac{\Delta t}{\phi \Delta V};$$

$$d_N^n = \frac{k_{22}\lambda_{w|_n}^n}{\Delta y_n}\rho_w g\frac{\Delta t}{\phi \Delta V}; \qquad d_S^n = \frac{k_{22}\lambda_{w|_s}^n}{\Delta y_s}\rho_w g\frac{\Delta t}{\phi \Delta V};$$

$$d_F^n = \frac{k_{33}\lambda_{w|_f}^n}{\Delta z_f}\rho_w g\frac{\Delta t}{\phi \Delta V}; \qquad d_B^n = \frac{k_{33}\lambda_{w|_b}^n}{\Delta z_b}\rho_w g\frac{\Delta t}{\phi \Delta V}; \qquad (A-9)$$

$$d_P^n = d_E^n + d_W^n + d_N^n + d_S^n + d_F^n + d_B^n \qquad (A-10)$$

Appendix B

B.1 Eclipse Model of Self-Constructed Case

```
RUNSPEC

DIMENS
   10   7   6/

NONNC

OIL
WATER

METRIC

TABDIMS
   1   1   15   15   1   15 /

WELLDIMS
   1   200   1   2 /
START
   14 'JAN' 2014  /

NSTACK
   25 /

--FMTOUT

--FMTIN

UNIFOUT

UNIFIN

--NOSIM

GRID    ================================================================

INIT
--     ARRAY  VALUE     ------- BOX ------
EQUALS
      'DX'    5      /
      'DY'    5      /
      'TOPS'  3535   /
      'PORO'  0.5    /

      'DZ'    5      /
      'PERMX' 1      /
      'PERMZ' 0.1      /
/

COPY
      'PERMX'    'PERMY'   /
/

RPTGRID
```

```
  1  1  1  1  1  1  0  0  1  1  0  1  1  0  1  1  1 /

PROPS    ================================================================

--      Sw kro
SOF2
       0.0 0.0
       0.0889    0.0
       0.1778    0.0
       0.2667    0.0
       0.3 0.0
       0.3556    0.0123
       0.4444    0.0835
       0.5333    0.2178
       0.6222    0.4153
       0.7191    0.6769
       0.8       1.0
/

--     Sw     krw       pcow
SWFN
     0.200    0.0      31.0264
     0.2809   0.0022   1.31207
     0.3778   0.0180   0.69430
     0.4667   0.0607   0.33784
     0.5556   0.1438   0.12410
     0.6444   0.2809   0.03447
     0.7000   0.4089   0.00345
     0.7333   0.4855   0.00069
     0.8222   0.7709   0.0000
     0.9111   1.0000   0.0000
     1.0000   1.0000   0.0000
/

PVTW
     1.014  1* 0.000041    0.3  0  /

PVDO
 100      1.02     1.0
 200      1.01     1.0
   /

ROCK
       1.014 0 /

--        OIL    WATER  GAS
DENSITY
         660.0   870.0   1* /

RPTPROPS
1  1  1  0  1  1  1  1  /

SOLUTION ================================================================
--    DATUM  DATUM   OWC    OWC    GOC    GOC    RSVD   RVVD   SOLN
--    DEPTH  PRESS  DEPTH   PCOW  DEPTH   PCOG  TABLE  TABLE   METH
EQUIL
       3535   140   3600 1* 3100 /
```

```
RPTSOL
   1  11*0  /

SUMMARY  ============================================================

RUNSUM

FLPT
FOPT
FPR
FLPR
FOPR

WBHP
'PRODUCER'
/
BPR
10 4 3
10 4 4
/

CPR
'PRODUCER' 10 4 3/
'PRODUCER' 10 4 4/
/

SCHEDULE ============================================================

RPTSCHED
   0 0 0 0 0 0 0 0 0 0
   0 2 0 0 2    /

IMPES
 1.0 1.0 10000.0 /

TUNING
.01  .01 0.001 /
1.0 0.5 1.0E-6 /
/
--     WELL   GROUP LOCATION  BHP   PI
--     NAME   NAME    I  J   DEPTH DEFN
WELSPECS
    'PRODUCER' 'W'   10 4    3538 'LIQ'  /
/
--     WELL     -LOCATION- OPEN/ SAT CONN  WELL
--     NAME     I  J K1 K2 SHUT  TAB FACT  DIAM
COMPDAT
    'PRODUCER'  10 4 3  4 'OPEN' 2*   0.5  /
  /
--      WELL     OPEN/  CNTL   OIL  WATER   GAS  LIQU   RES   BHP
--      NAME     SHUT   MODE  RATE   RATE  RATE  RATE  RATE
WCONPROD
     'PRODUCER' 'OPEN' 'BHP'  5* 100  /
  /

TSTEP
 .05 .2 50*2.0
  /
```

```
RPTSCHED
 1 1 1 1 1 0 2 1 2 0
 2 2 0 0 2 /

TSTEP
 2.5
  /

END     ============================================================
```

B.1 Eclipse Model SPE Five-Spot Quarter

```
RUNSPEC

TITLE
 THIS LINE IS A RUN TITLE

DIMENS
    5    5    1  /

OIL

WATER

FIELD

TABDIMS
    1    1   20    2    1   20 /

WELLDIMS
    1    1    1    2 /

START
   1 'JAN' 1983  /

NSTACK
    8 /

FMTOUT

FMTIN

GRID      ============================================================
INIT

DXV
   5*75.0 /

PERMX
  25*50.0 /

PERMY
  25*50.0 /

DYV
   5*75.0 /

DZ
  25*30.0 /

TOPS
  25*4000.0 /

PERMZ
  25*50.0 /

PORO
  25*0.2 /
```

```
RPTGRID
-- Report Levels for Grid Section Data
--
'DX'
'DY'
'DZ'
'PERMX'
'PERMY'
 /

PROPS     ================================================================

SWFN
    .25    .0    4.0
    .7    1.0     .0
/

SOF2       1 TABLES   20 NODES IN EACH           FIELD   13:34  5 MAY 85
    .3000  0.0000
    .7500  1.0000
/

PVTW
  .0  1.0  3.03E-06  .5  0.0 /

PVDO
  .0     1.0     2.0
 8000.0   .92    2.0
/

ROCK
 4000.0         .30E-05 /

DENSITY
 52.0000  64.0000   .04400 /

RPTPROPS
     /

REGIONS    ================================================================

SATNUM
 25*1 /

SOLUTION   ================================================================

EQUIL
4000  4000  6000  0   0   0   0   0   0  /

RPTSOL
-- Initialisation Print Output
--
'PRES' 'SWAT' /

SUMMARY    ============================================================

BPR
```

```
1 1 1
/

FOPR

WBHP
/

FWCT

FPR

SCHEDULE   ============================================================

RPTSCHED                                          FIELD   16:55 18 APR 86
 'PRES' 'SWAT' 'RESTART=1' 'CPU=2' /

WELSPECS
--'I'  'G'   1  1  4000  'WAT'  /
'P'  'G'   5  5  4000  'OIL'  /
/

COMPDAT
--'I       '   1   1   1   1 'OPEN'   0  .0   1.0 /
'P       '   5   5   1   1 'OPEN'   0  .0   1.0 /
/

WCONPROD
'P' 'OPEN' 'BHP' 5* 3500.0 /
/

--WCONINJE
--'I' 'WAT' 'OPEN' 'RATE' 200.0 /
/

TSTEP
 4*25
/

END
```